Atmos. Meas. Tech. Discuss., https://doi.org/10.5194/amt-2017-214
Manuscript under review for journal Atmos. Meas. Tech.
Discussion started: 17 July 2017

Atmospheric Measurement Techniques Discussions

GARRLiC and LIRIC: strengths and limitations for the characterization of dust and marine particles along with their mixtures

Alexandra Tsekeri[1], Anton Lopatin[2], Vassilis Amiridis[1], Eleni Marinou[1,3], Julia Igloffstein[4], Nikolaos Siomos[3], Stavros Solomos[1], Panagiotis Kokkalis[1], Ronny Engelmann[4], Holger Baars[4], Myrto Gratsea[5], Panagiotis I. Raptis[5,6], Ioannis Binietoglou[7], Nikolaos Mihalopoulos[5,8], Nikolaos Kalivitis[1,8], Giorgos Kouvarakis[8], Nikolaos Bartsotas[9], George Kallos[9], Sara Basart[10], Dirk Schuettemeyer[11], Ulla Wandinger[4], Albert Ansmann[4], Anatoli P. Chaikovsky[12], and Oleg Dubovik[2]

[1]{Institute for Astronomy, Astrophysics, Space Applications and Remote Sensing, National Observatory of Athens, Athens, Greece}

[2]{Laboratoire d' Optique Atmosphérique, Universite de Lille, Lille, France}

[3] {Laboratory of atmospheric physics, Physics Department, Aristotle University of Thessaloniki, Greece}

[4]{Leibniz Institute for Tropospheric Research, Leipzig, Germany}

[5]{IERSD, National Observatory of Athens, Athens, Greece}

[6]{Physikalisch-Meteorologisches Observatorium Davos/World Radiation Center (PMOD/WRC), Davos Dorf, Switzerland}

[7]{National Institute of R&D for Optoelectronics, Magurele, Ilfov, Romania}

[8]{Environmental Chemical Processes Laboratory, University of Crete, Heraklion, Greece}

[9]{University of Athens, School of Physics, Athens, Greece}

[10]{Barcelona Supercomputing Center, Barcelona, Spain}

[11]{European Space Agency}

[12]{Institute of Physics, NAS of Belarus, Minsk, Belarus}

Correspondence to: Alexandra Tsekeri (atsekeri@noa.gr)

Atmos. Meas. Tech. Discuss., https://doi.org/10.5194/amt-2017-214
Manuscript under review for journal Atmos. Meas. Tech.
Discussion started: 17 July 2017

Atmospheric Measurement Techniques Discussions

Abstract

The **G**eneralized **A**erosol **R**etrieval from **R**adiometer and **Li**dar **C**ombined data algorithm (GARRLiC) and the **LI**dar-**R**adiometer **I**nversion **C**ode (LIRIC) provide the opportunity to study the aerosol vertical distribution by combining ground-based lidar and sun-photometric measurements. Here, we utilize the capabilities of both algorithms for the characterization of Saharan dust and marine particles, along with their mixtures, in the South-Eastern Mediterranean during the "**CHAR**acterization of **A**erosol mixtures of **D**ust and **M**arine origin **Exp**eriment (CHARADMExp)". Three case studies are presented, focusing on dust-dominated, marine-dominated and dust/marine mixing conditions. GARRLiC and LIRIC achieve a satisfactory characterization for the first case in terms of particle microphysical properties and concentration profiles. The marine-dominated and the mixture cases are more challenging for both algorithms, although GARRLiC manages to provide more detailed microphysical retrievals compared to AERONET, while LIRIC effectively discriminates dust and marine in its concentration profile retrievals.

1 Introduction

The importance of studying the vertical distribution of aerosol plumes is prominent in regional and climate studies, since it can effectively change the radiative properties of the atmosphere and the presence of clouds (e.g. Pérez et al., 2006a; Solomon et al., 2007). Ground-based monitoring of the aerosol vertical structure is effectively performed with the synergy of passive and active remote sensing instruments, in particular with multi-wavelength sun-photometers and lidars. The sun-photometer provides the columnar properties of the particles (e.g. Dubovik and King, 2000a; Dubovik et al., 2006), whereas the lidar is capable of providing vertical profiles of the backscatter and extinction coefficients, along with vertical profiles of the particle microphysical properties, mainly for the fine mode (e.g. Müller et al., 2015). The combination of active with passive remote sensing has been tried so far mainly by using the sun-photometer measured aerosol optical depth (AOD) as ancillary information for the lidar retrieval (e.g. Fernald et al., 1972; Ansmann et al., 2011; 2012). GARRLiC (Lopatin et al., 2013) and LIRIC (Chaikovsky et al., 2016) algorithms go a step further and use deeper synergies: the LIRIC approach derives the particle concentration profiles from the lidar measurements, considering the columnar microphysical properties derived separately from the sun-photometer; GARRLiC

advances the method even more, combining for the first time both sun-photometer and lidar measurements for the retrieval of the particle microphysical properties. As discussed in detail in Lopatin et al. (2013), combining the sun-photometer intensity measurements with the backscatter lidar information seems to result in better sensitivity to the particle shape, as well as the ability to retrieve the refractive indices of fine and coarse particles separately, along with extracting the vertical distribution of the fine and coarse particle concentrations. Moreover, it can potentially provide higher accuracy for cases of low aerosol loadings, compared with the intensity-only retrieval.

GARRLiC and LIRIC have been developed in the framework of the Aerosols, Clouds and Trace gases Research Infrastructure (ACTRIS, http://www.actris.eu/), utilizing the capabilities of combined European stations of the AErosol RObotic NETwork (AERONET, Holben et al., 1998) and the European Aerosol Research Lidar Network (EARLINET, Pappalardo et al., 2014). Both algorithms have been tested for a variety of aerosol types and their mixtures. For example, LIRIC has been tested for dust and volcanic aerosols (Wagner et al., 2013), dust/pollution mixture (Tsekeri et al., 2013), dust, pollution and mixture of dust/smoke and pollution (Granados-Muñoz et al., 2014; 2015; Papayannis et al., 2014), and smoke/pollution mixture (Kokkalis et al., 2016). LIRIC has also been used to study dust transport events and dust modeling performance over Europe (Binietoglou et al. 2015, Granados-Munoz, 2016), as well as to evaluate air quality models (Siomos, et al. 2017). GARRLiC has been tested for dust and smoke (Lopatin et al., 2013) and dust aerosols (Bovchaliuk et al., 2016).

GARRLiC and LIRIC input and output data is shown in Fig. 1, while short descriptions are given herein: LIRIC algorithm uses the particle microphysical properties provided in the AERONET product as a-priori information in the inversion of the lidar measurements for retrieving the aerosol volume concentration profiles. Using lidar measurements of elastic backscatter at three wavelengths of 355, 532, and 1064 nm, LIRIC retrieves the volume concentration profiles of fine and coarse particles, whereas considering also the cross-polarized lidar signal at 532 nm the coarse mode can be disentangled into its spherical and non-spherical components. The error estimation of the retrieved profiles is provided as well. Both LIRIC and GARRLiC retrievals assume that key aerosol properties vary smoothly (e.g. aerosol concentration varies smoothly with height), but otherwise do not constrain the absolute values of the retrieved quantities. In this way the algorithms exclude solutions that are mathematically possible, but contain unrealistic oscillations in the retrieved properties (see also Dubovik, 2004;

Dubovik and King, 2000). GARRLiC algorithm combines the sun-photometer sun and sky measurements at four wavelengths (at 440, 670, 870 and 1020 nm) and up to 35 scattering angles, with the vertically-resolved lidar measurements of the elastic backscatter at three wavelengths (at 355, 532, and 1064 nm). The algorithm calculates the size distribution, spherical particle fraction and spectral complex refractive index, separately for fine and coarse particles, considering them constant along the atmospheric column, and the volume concentration profiles of fine and coarse particles. The retrieval uncertainties of the microphysical parameters are provided as well, and the profile retrieval uncertainties are currently under development. The volume concentration below the lowest height of the lidar signals is considered to be constant. Moreover, in case of a dominant mode (e.g. for pure dust cases), the algorithm is set to retrieve the aerosol characteristics for one mode only. GARRLiC and its updates are available for download at http://www.grasp-open.com/doc/ch04.php#grasp-manager, as part of the GRASP code (Dubovik et al., 2014).

In case of multi-mode aerosol mixtures an inherent deficiency of both algorithms is the number of aerosol modes retrieved, with LIRIC considering three modes (fine particles, coarse spherical and coarse non-spherical particles) and GARRLiC considering two modes (fine and coarse particles). We need to highlight here that LIRIC retrieves three modes only for the volume concentration profiles, whereas otherwise it uses the AERONET products, providing for example a common spectral refractive index for all modes (Fig. 1). Both algorithms work well for individual aerosol components or mixtures of (mainly) fine (e.g. pollution) and (mainly) coarse (e.g. dust) particles, but they should not be able to fully characterize the mixture components in case of more than one fine or coarse mode in the mixture, as in smoke/pollution or dust/marine mixture cases. For the latter, LIRIC should provide an effective characterization for the volume concentration profiles, since it derives the coarse spherical (hydrated marine) particles and the non-spherical (dust) particles, but the characterization is not expected to be satisfactory for the particle microphysical properties.

In our study, we apply GARRLiC and LIRIC for cases of dust, marine and dust/marine mixture during the CHARADMExp campaign in the South-Eastern Mediterranean. This is the first time a detailed characterization of marine and marine mixtures with dust along the atmospheric column is performed for the area. So far, various studies have tried to characterize the aerosol radiative properties in the Mediterranean with satellite or ground-based AOD measurements (e.g. di Sarra et al., 2008; Kazadzis et al., 2009; Papadimas et al., 2012). Unfortunately, they

fail to overcome their limitations such as the non-realistic assumptions for the aerosol absorption properties and the lack of information of the real vertical aerosol structure (Mishra et al., 2014). The kind of characterization presented here is important for application in future satellite missions not only for the Mediterranean, but for large parts of the globe where dust and marine particles are present, as in the Atlantic Ocean (e.g. Prospero, 1996).

The CHARADMExp campaign and the three cases (i.e. mainly dust, marine/pollution mixture and dust/marine/pollution mixture) are presented in section 2. The methodology followed in our work is presented in section 3, the GARRLiC and LIRIC results are shown in section 4 and finally our conclusions are given in section 5.

2 Overview of the CHARADMExp campaign and datasets

CHARADMExp was an experimental campaign of ESA, implemented by the National Observatory of Athens (NOA), aiming at the characterization of dust and marine particles along with their mixtures (http://charadmexp.gr). The campaign took place at the ACTRIS Finokalia station (35.338°N, 25.670°E) on the north coast of Crete, in Greece (Fig. 2), from 20 June to 20 July 2014. The station is situated at the top of a hilly elevation (252 m above sea level) and it is a background site with no human activities occurring at a distance shorter than 15 km, making the station ideal for monitoring natural aerosols mainly of desert and marine origin. The area is characterized by the existence of two well-distinguished seasons equally distributed throughout the year: the dry season from April to September and the wet season from October to April, with the first one characterized mainly by winds of N/NW direction (Central and Eastern Europe and Balkans) carrying smoke and long range transported anthropogenic pollution to the area (Sciare et al., 2008; Vrekoussis et al., 2005), and the second one with less pronounced N/NW winds and important transport from the Sahara desert (S/SW winds; occurrence up to 20%). Dust transport is less frequent during the dry period, however commonly observed (e.g. Papadimas et al., 2005), characterized by a transportation pattern through the free troposphere and weaker vertical mixing of the dust layers (e.g. Kalivitis et al., 2007).

Atmos. Meas. Tech. Discuss., https://doi.org/10.5194/amt-2017-214
Manuscript under review for journal Atmos. Meas. Tech.
Discussion started: 17 July 2017

2.1 Instruments and methods

2.1.1 Lidar

The Polly^{XT} OCEANET lidar (Engelmann et al., 2016) operated at a 24/7 basis during CHARADMExp, measuring aerosol loads in the boundary layer and the free troposphere. The system was provided by the Leibniz Institute for Tropospheric Research (TROPOS - http://www.tropos.de). It employs 3 backscatter channels (at 355, 532 and 1064 nm), 2 Raman extinction channels (at 387 and at 607 nm), 2 depolarization channels (at 355 and 532 nm) and one water–vapor channel (at 407 nm). The lidar is housed in a container and can be operated under various climatic conditions. The full description of the original lidar system can be found in Althausen et al. (2009) and in Engelmann et al. (2016). More about the network of Polly systems (i.e., Polly^{NET}) can be found in Baars et al. (2016).

The information close to the surface is very important for our study, especially for the marine particle characterization, since the marine particles reside mostly below 1 km (e.g. Ho et al., 2015). Unfortunately, this is also the lidar "overlap region", with large uncertainty for the lidar backscattered signal due to its partial collection from the telescope (e.g. Wandinger and Ansmann, 2002). Polly^{XT} OCEANET far-field (FF) signal full overlap is at ~800 m (Engelmann et al., 2016) and it operates two near–field (NF) channels utilizing a separate 50–mm refractor telescope at a distance of 120 mm from the axis of the laser beam, providing a full overlap at 150 m above surface at 532 and 607 nm. The NF measurements are not used in the input of GARRLiC and LIRIC, since both algorithms require the complete set of wavelengths provided by the lidar during CHARADMExp only for the FF measurements. Nevertheless, we use the NF measurements to perform overlap correction in the FF signals, as described in Engelmann et al. (2016), and this allowed us to use the FF-corrected lidar signals from ~550 m, instead of 800 m. In future efforts we plan to utilize the additional information provided by our new Polly^{XT} lidar system currently installed at Finokalia station, measuring NF signals at both 355 and 532 nm, by performing the signal gluing technique for NF and FF signals at 355 and 532 nm and overlap correction for the FF signal at 1064 nm.

2.1.2 Sunphotometer

The CIMEL CE318 sunphotometer is the instrument used in the AERONET sunphotometer network, with more than 250 units worldwide. The technical specifications of the instrument are given in detail by Holben et al. (1998). Taking into account all the information about the

instrument precision and calibration precision (Holben et al., 1998) the accuracy of the AOD measurements is estimated to be of the order of ±0.02 in the UV and ±0.01 in the Visible regarding the level 2 (cloud-screened and quality-assured) data. In the current analysis we utilized the level 1.5 products (i.e., automatically cloud cleared but may not have final calibration applied) for the LIRIC retrieval, since the level 2 data were not available in the time ranges selected for the retrievals. For the GARRLiC retrieval we used the sun and sky multi-angle measurements at four wavelengths (440, 670, 870 and 1020 nm) (Dubovik and King, 2000).

2.1.3 Surface in situ

The GARRLiC retrieved size distribution is evaluated against the surface measurements of the Scanning Mobility Particle Spectrometer (SMPS). SMPS provides the fine particle number size distribution at ~9 - 848 nm (nominal) radius. Unfortunately, there were no size distribution measurements for the coarse particles at Finokalia station during CHARADMExp. Note that for a direct comparison of SMPS number size distribution (in cm^{-3}) with the GARRLiC volume size distribution retrievals (in $\mu m^3 \mu m^{-2}$) we first have to calculate the SMPS volume size distribution (in $\mu m^3 cm^{-3}$) and then to multiply it with the extent of fine particles in the column, derived by the collocated lidar measurements.

Moreover, we evaluate the particle concentration derived from GARRLiC and LIRIC at the surface level with the surface in situ measurements of the particular matter for particles with diameters less than 10 μm (PM_{10}). The PM_{10} is continuously measured at Finokalia station with an Eberline FH 62 I-R (Eberline Instruments GmbH) particulate monitor (Gerasopoulos et al., 2006). GARRLiC and LIRIC retrieve the particle concentration for a wider size range (up to 15 μm in radius, or 30 μm in diameter), thus their PM_{10} values are calculated using the respective volume percentages for particles with radius less than 5 μm.

In order to compare the in situ measured size distribution and mass concentration with GARRLiC and LIRIC ambient retrievals, we need to take into account the particle drying applied to surface measurements. The in situ instruments dry the sampled air by adiabatic compression during the sampling through their inlets and by the radiant heat from the lights inside the instruments. The size and mass of the ambient particles thus changes, especially in case of hygroscopic particles in humid conditions (e.g. Snider and Petters, 2008). For the size distribution we evaluate this effect qualitatively (see section 4.2 and 4.3). For the PM_{10}

Atmos. Meas. Tech. Discuss., https://doi.org/10.5194/amt-2017-214
Manuscript under review for journal Atmos. Meas. Tech.
Discussion started: 17 July 2017

comparison we calculate the "dry" GARRLiC and LIRIC PM_{10}, using the particle hygroscopic growth (i.e., the ratio of the ambient to dry particle size, f_g) as shown in Eq. 1:

$$PM_{10_d} = f_g^{-3} PM_{10_a} \quad (1)$$

where d and a denote the dry and ambient particles, respectively.

We derive f_g for different relative humidity (RH) values using the hygroscopicity parameter κ (Petters and Kreidenweis, 2007) as shown in Eq. 2:

$$f_g = \left(1 + \kappa \frac{RH}{100 - RH}\right)^{\frac{1}{3}} \quad (2)$$

For the cases analysed herein, we consider a κ value of 0.4 to be characteristic for particles in the south-eastern Aegean Sea (Bezantakos et al., 2013). A more detailed treatment of comparing dry in situ measurements with ambient remote sensing retrievals is out of the scope of this analysis, but it is very important when combining these different techniques (e.g. Tsekeri et al., 2017).

2.2 Models

2.2.1 Source-receptor analysis

The origin of the examined aerosol layers at the Finokalia station is investigated with the use of source-receptor computations derived with dispersion modelling tools. The corresponding emission sensitivity (i.e. the residence time of the tracer particles inside the lowest tropospheric layers) is calculated from backward Lagrangian simulations with the atmospheric dispersion model FLEXPART-WRF (Brioude et al., 2013). The dispersion model is offline coupled with the WRF_ARW atmospheric model (Skamarock et al., 2008). The spatial resolution of WRF is 12×12 km and we use its hourly outputs to drive the FLEXPART runs. This configuration allows the simulation of meso-γ scale circulations that play an important role for the planetary boundary layer properties and for the regional and local scale transport of the particles. The backward FLEXPART runs are performed for 5-day periods and we assume a release of 40000 tracer particles from each arriving layer over the Finokalia station. The modelled retroplume maps show the spatial distribution of the tracer particle residence time below 1 km. Thus, the areas showing longer residence times in these maps indicate the source areas/origin of the particles arriving at the specific heights above Finokalia station.

Atmos. Meas. Tech. Discuss., https://doi.org/10.5194/amt-2017-214
Manuscript under review for journal Atmos. Meas. Tech.
Discussion started: 17 July 2017

2.2.2 Desert dust model

Desert dust emissions and transport are described with the BSC-DREAM8b model (Nickovic et al., 2012; Pérez et al., 2006a; Basart et al., 2012a). The BSC-DREAM8b model is embedded into the Eta/NCEP atmospheric model and solves the mass balance equation for dust, taking into account the different processes of the dust cycle (i.e., dust emission, transport and deposition). The updated version of the model includes a source function based on the 1 km USGS land use data, 8 particle size bins (0.1–10 μm radius range), and dust-radiative feedbacks.The present analysis utilize the BSC-DREAM8b dust simulations for the period from 20 June to 20 July 2014 with hourly output. The initial state of dust concentration in the model is defined by the 24 h forecast from the previous day model run. The NCEP Final Analyses (at 1º × 1º horizontal resolution) at 00:00 UTC are used as initial conditions and boundary conditions at intervals of 6 h. Moreover, the model configuration includes 24 Eta vertical layers extending up to approximately 15 km in the vertical. The resolution is set to 1/3° in the horizontal.

2.2.3 Sea-salt model

Sea salt emissions and transport are described with the atmospheric model RAMS-ICLAMS (Solomos et al., 2011). The model is an enhanced version of RAMS (Pielke et al., 1992; Cotton et al., 2003) and it includes a full description of the sea salt lifecycle in the atmosphere. The parameterization of sea salt emission is based on the white-cap formation for the entrainment of sea salt spray in the atmosphere (Monahan et al., 1986), taking also into account the effects of RH on the size distribution of the particles (Zhang et al. 2005). Sea salt flux close to the coastline is also calculated in the model following the parameterizations of Leeuw et al. (2000) and Gong et al. (2002). The dry and wet removal processes are treated with the corresponding schemes described in Seinfeld and Pandis (1998). The simulated sea salt mass is represented with a bimodal lognormal distribution. The first (accumulated) mode has a mean diameter of 0.36 μm and a geometric dispersion of 1.80. The second (coarse) mode has a mean diameter of 2.85 μm and the geometric dispersion is 1.90.

3 Results

In order to demonstrate the GARRLiC and LIRIC capabilities in characterizing events with dust and marine particles, we analyse in detail three cases acquired during CHARADMExp at

Finokalia. The first case is a relatively moderate dust episode with low amount of marine and continental particles, the second is a low-AOD marine and continental plume and the last is a mixture of dust, marine and continental particles. Source-receptor simulations are used to derive the particle origin and characterize the air masses. Then, we compare the optical properties retrieved from GARRLiC and LIRIC, as well as the collocated Klett retrievals (Klett, 1985). The GARRLiC and LIRIC/AERONET fine mode size distributions and PM_{10} concentrations are compared with surface in situ measurements. Finally, the dust and marine concentration profiles are compared with the corresponding profiles from BSC-DREAM8b and RAMS-ICLAMS models.

3.1 Dust-dominated case

On June 26 the Polly^{XT} measurements of volume depolarization ratio at 532 nm showed the advection of non-spherical particles (volume depolarization ratio at 532 nm of 0.15-0.2), at height ranges extending from close to the ground up to 5-6 km (Fig. 3a) and an AOD at 440 nm of 0.4. Model simulations also support our observations: dust transport simulations using the BSC DREAM8b model indicate Saharan dust transport to Finokalia. As shown by the FLEXPART footprints in Fig. 3b, the particles reaching from the ground up to 2 km have possible near-surface sources at the West Sahara region, with potential mixing of marine and continental particles from the western Mediterranean region, the Balkans and Greece, while the particles arriving at 3-6 km are most likely dust from the Sahara desert between 0°-10° E and 25°-35° N. The presence of dust particles is indicated from AERONET as well, with Ångstrom exponent at 440/870 nm of ~0.1, sphericity parameter <2.3 % and a coarse-mode dominated size distribution. These values are characteristic for dust particles, as reported in the 8-year global AERONET climatology of Dubovik et al. (2002).

Considering that the atmospheric column is dominated by dust (as shown in the coarse mode dominated AERONET size distribution), we performed the one-mode GARRLiC inversion. For both GARRLiC and LIRIC we used the lidar measurements at 4-6 UTC (red box in Fig. 3a) and the sun-photometer measurements at 4:54 UTC. Our results show that GARRLiC and LIRIC backscatter and extinction coefficient profiles at 355, 532 and 1064 nm agree quite well within the LIRIC uncertainties with small differences seen below ~550 m, in the lidar incomplete overlap region (first and second row in Fig. 4). Figure 4 shows also the comparison of GARRLiC backscatter and extinction coefficients with the ones produced with the Klett

method (Klett, 1985). The Klett profiles are cut above 5 km, since the low signal to noise ratio of the day-time lidar measurements introduces large uncertainty to the Klett retrievals above that height. For the Klett retrievals we used an extinction-to-backscatter ratio, or "lidar ratio" (LR) of 40 sr for 532 and 1064 nm and of 47 sr for 355 nm, which result in extinction coefficient profiles that closely reproduce the sun-photometer-measured AODs at 340, 500 and 1020 nm (i.e. 0.42, 0.42 and 0.38), respectively. The uncertainty in the assumed lidar ratios are taken into account by considering a 20 % uncertainty in the backscatter retrievals (Fig. 4, third row). The agreement of GARRLiC with Klett retrievals is considered satisfactory, with differences for the backscatter coefficient to be within the Klett retrieval uncertainty, and for the extinction coefficient to be less than 30% at heights above 550 m. Figure 4 shows also the NF retrievals at 532 nm, providing information of the particle properties down to 150 m: In particular, we see a decrease in the particle backscatter and extinction coefficients near the surface, which is not retrieved by GARRLiC or LIRIC due to missing NF information as discussed in section 3.1.1.

A special feature seen in GARRLiC, LIRIC and Klett backscatter profiles is the larger backscatter at 532 than 355 nm. This is not usual for dust particles, but it has been reported before: Veselovskii et al. (2016) have shown a similar spectral dependence for dust during the study of SaHAran Dust Over West Africa (SHADOW) campaign, which they attributed to large dust particle spectral variation of the imaginary part of the refractive index. More specifically, they managed to reproduce this backscatter spectral dependence with imaginary part values of 0.005-0.05 at 355 nm and 0.005 at 532 nm. Although these values are not the same with the retrieved 0.001 at 355 nm and 0.0005 at 532 nm for our case (Fig. 5 –bottom, right), the backscatter spectral dependence can be a combination of the effect that different factors have on the backscattered light, as the size, shape or orientation of the dust particles.

Figure 5 shows good agreement between GARRLiC and AERONET retrievals (the latter used in the LIRIC retrieval), within the GARRLiC retrieval uncertainties. Differences are seen only for the real part of the refractive index, which for GARRLiC is at ~1.45, at the low end of the dust climatological value range of 1.48±0.05-1.56±0.03 as reported in Dubovik et al. (2002). This value though is much lower than expected for dust from West Sahara in situ measurements, reporting values of 1.55-1.65 (e.g. Kandler et al., 2007), and it may be due to the marine particle mixture at lower heights, with real part of refractive index of ~1.35. An important feature of the GARRLiC retrieval is the spectral dependence of the single scattering albedo (SSA), showing

the characteristic increase of dust absorption in the ultraviolet (Fig. 5, up right) (Otto et al., 2007). Moreover, the GARRLiC size distribution agrees well with surface in-situ SMPS measurements for the fine mode, showing a very small volume concentration for fine particles. The SMPS number size distribution is converted to $\mu m^3 \mu m^{-2}$ for a direct comparison with the GARRLiC and AERONET product, as described in section 2.1.3: For this conversion we consider that mainly the first 2 km contain fine particles due to the mixing of marine and continental particles with dust there (Fig. 3b). Moreover, due to the low RH at the surface of 16%, we do not expect differences between the GARRLiC ambient size distribution and the SMPS dry measurements.

The concentration profiles from GARRLiC and LIRIC are in excellent agreement at heights >1 km (Fig. 6a). LIRIC retrieves fine and coarse mode profiles, whereas GARRLiC considers only one mode, dominated by coarse particles. The LIRIC coarse mode is comprised only of non-spherical particles. Figure 6b (left) shows the comparison of GARRLiC and LIRIC dust particle profiles with the BSC DREAM8b model. For this comparison we consider all particles in GARRLiC and LIRIC profiles to be dust particles. Furthermore, we multiply them with the dust density of 2.6 g cm^{-3} (Reid et al., 2003) to convert the volume concentration ratio (in ppb) to dust mass concentration (in $\mu g\, m^{-3}$). Although the shapes agree well, the BSC DREAM8b model values are lower than GARRLiC and LIRIC, by a factor of 2. The BSC DREAM8b underestimation when comparing to LIRIC is consistent with the findings of Binietoglou et al. (2015) for relative low dust concentrations (as is the case here). The underestimation is shown in the BSC DREAM8b dust AOD at 550 nm as well, with a value of ~0.2, which is half of the sun-photometer-measured AOD at 500 nm, of 0.4. When we scale the BSC-DREAM8b concentration with these AOD values (multiplying by a factor of 2) the bias is reduced to less than 10% at 1 km and 50% at 3 km, relative to GARRLiC and LIRIC concentrations. The GARRLiC and LIRIC mass concentrations are compared also with surface in situ PM_{10} measurements, showing the algorithms overestimating the particle concentration at the surface level (Fig. 6b, right). We calculate the PM_{10} concentrations from GARRLiC and LIRIC mass concentrations, as percentages of the particles with diameter less than 10 μm (i.e., 83% and 80% of the total mass, respectively). Figure 6b (right) shows the GARRLiC and LIRIC PM_{10} surface values (purple stars in plot), considering marine instead of dust particles at the surface, thus using the marine particle density for the volume to mass conversion (i.e., 1.7 g cm^{-3} for dry marine particles (Stock et al., 2011), since the measured RH at the surface is 16%). The

agreement with the surface in situ measurements is better now, but it is only indicatory, since what we have at the surface is most probably a mixture of marine, continental and dust particles as shown in Fig 3b.

Summarizing, the GARRLiC and LIRIC retrievals are performing well for the dust episode on July 26, considering the consistency with the Klett retrievals, the BSC DREAM8b modelled mass concentration profiles, the surface in situ measurements of the fine mode size distribution, as well as the expected increase of the dust absorption in the ultraviolet. The discrepancies seen for the retrieval closer to the surface and the PM_{10} at the surface level can be explained if we consider the incomplete lidar information in the overlap region.

3.2 Marine and polluted continental particle case

On July 15 the lidar measurements at 12:30-14:30 UTC showed a low-AOD layer of non-depolarizing particles, extending up to 3 km (Fig. 7a). The lack of depolarization indicates spherical (hydrated) marine particles which is also supported by our source-receptor analysis (Fig. 7b). Specifically, FLEXPART-WRF simulations show that the particles above Finokalia station have mainly a marine origin along the whole atmospheric column, with a possible contribution of continental aerosol from Southern Italy. This scenario is further supported by AERONET measurements at 13:24 UTC, of low AOD of ~0.06 at 500 nm, high Ångstrom exponent of ~1.2 at 440/870 nm and low refractive index of ~1.4+i0.0005 at 440 nm, which are within the climatological value ranges for marine particles and their mixtures, as reported from Dubovik et al. (2002).

The low AOD is unfavourable for the GARRLiC and AERONET microphysical property retrievals, especially for the spectral refractive index and SSA (Dubovik et al., 2000b; Lopatin et al., 2013). The latter require an AOD of at least 0.4 at 440 nm for satisfactory accuracy in case of sun-photometer-only retrieval (Dubovik et al., 2000b). The lidar information combined with the sun-photometer measurements in GARRLiC is expected to improve the retrieval in low AOD cases (Lopatin et al., 2013). Although the AOD requirements have not been quantified yet for GARRLiC, an AOD of 0.3 at 440 nm is considered sufficient. As reported in Dubovik et al. (2002) though, the marine particles rarely exceed the AOD of 0.15 at 440 nm, thus we do not expect highly accurate refractive index and SSA retrievals from GARRLiC, or from AERONET/LIRIC, for the marine particles. Even more so, the marine case analysed here has a much lower AOD, thus we consider the refractive index and SSA retrievals to be only

indicative for this case. In addition, as seen in Fig. 7a, most of the aerosol load is located below 1 km, where the lidar incomplete overlap region is located, which challenges even more the combined lidar/sun-photometer retrieval.

The GARRLiC and LIRIC retrievals used the lidar measurements at 12:30-14:30 UTC (red box in Fig. 7a) and the sun-photometer measurements at 13:24 UTC. Figure 8 shows the retrieved backscatter and extinction coefficients at 355, 532 and 1064 nm, and the corresponding retrievals from the Klett method. For the latter we consider a LR of 50, 45 and 45, for 355, 532 and 1064, respectively, that closely reproduce the sun-photometer measured AODs of 0.1, 0.05 and 0.02 at 340, 500 and 1020 nm. The agreement between GARRLiC and LIRIC is satisfactory within the LIRIC uncertainties. Above 550 m, this is also the case for GARRLiC and Klett backscatter coefficient retrievals, whereas for the extinction coefficients the differences are within 30% for 355 nm and 10-40% for 532 nm relative to GARRLiC values. In the marine boundary layer (below 550 m) the Klett NF backscatter and extinction coefficients at 532 nm show much larger values than the ones retrieved from GARRLiC and LIRIC. This highlights very vividly the importance of the NF measurements in properly retrieving the marine particle properties with lidars.

GARRLiC retrieves both fine and coarse particles in this case, which we consider to be mainly of continental and marine origin, respectively. The fine particle volume size distribution shows ~10% more volume than the AERONET product (also used in LIRIC retrieval), as well as the surface in situ SMPS measurements (Fig. 9, up left). The SMPS volume size distribution is converted to $\mu m^3 \mu m^{-2}$ considering that most particles reside from the surface up to ~ 1 km (Fig. 7). The difference may be partly due to the instrument drying the particle sample, but the effect is not expected to be that strong since the RH at the surface is 60% and the corresponding hygroscopic growth is estimated at 1.17 (section 2.1.3, Eq. 2). For the coarse mode, GARRLiC retrieves ~50% more volume than AERONET. The AERONET SSA and spectral refractive index retrievals are the same with the GARRLiC fine mode retrievals, or within the retrieval uncertainty (Fig. 9). These high values of SSA (close to 1) and the refractive index of 1.38±0.4+i0.0005±0.0003 are within the range of climatological values of continental particles, according to Dubovik et al. (2002). For the GARRLiC coarse mode, the SSA and imaginary part of the refractive index show very high values for marine particles, which are most probably false, whereas the real part of the refractive index of ~1.36 agrees well with the climatological value of 1.36±0.01 for marine particles (Dubovik et al., 2002).

Figure 10a shows the GARRLiC and LIRIC volume concentration profiles, which agree well within the LIRIC retrieval uncertainties above 550 m, whereas below the GARRLiC concentration for the coarse particles is larger. Assuming that the marine particles are comprised only of coarse particles, we derive the marine mass concentration profiles from GARRLiC and LIRIC as shown in Fig. 10b (left). The mass concentration profiles are calculated from the coarse volume concentration profiles using a sea salt density of 1.3 g cm^{-3}. This value denotes the density of a sea salt solution at a RH of 50-60 % (Eq. 3 in Zhang et al. (2005)), with the RH values provided from the RAMS model. Figure 10b (left) shows also the RAMS-ICLAMS sea salt model mass concentration profile which presents lower values than GARRLiC and LIRIC, with differences of ~80% and 60% at the surface, respectively. Moreover, GARRLiC and LIRIC PM_{10} mass concentrations seem to agree well with the surface in situ PM_{10} measurements (Fig. 10b, right), within the time variability of the latter. The GARRLiC and LIRIC PM_{10} values are calculated using the respective percentages of volume size distributions for particles with diameter less than 10 μm (i.e., the sum of fine mode volume and 35% of coarse mode volume for GARRLiC and 50% of total volume for AERONET/LIRIC). The comparison with the in situ measurements should also consider the drying of the ambient sample by the in situ instrument. We calculate the GARRLiC and LIRIC "dry" PM_{10}, considering a hygroscopic growth factor of 1.17 at RH=60% at the surface (section 2.1.3). The "dry" values agree well with the in situ measurements, within the latter time variability.

Summarizing, GARRLiC retrieves more fine particles than AERONET and surface in situ measurements. The fine particle SSA and refractive index is characteristic of continental particles. The corresponding coarse mode retrieval probably fails for SSA and the imaginary part of the refractive index, which are very difficult to be retrieved with low AODs, but the real part of the refractive index properly assigns the refractive index of marine particles. Both GARRLiC and LIRIC concentration profiles seem to agree well with the PM_{10} surface in situ measurements. Since the marine-dominated scenes usually have very low AOD and low vertical extent (Ho et al., 2015), it is challenging to obtain trustworthy retrievals from GARRLiC and LIRIC for marine particle scenes. One way to improve the marine retrievals in future efforts could be to try to increase the lidar information in the overlap region, utilizing for example the NF lidar measurements, as discussed in section 3.1.1.

Atmos. Meas. Tech. Discuss., https://doi.org/10.5194/amt-2017-214
Manuscript under review for journal Atmos. Meas. Tech.
Discussion started: 17 July 2017

3.3 Dust and marine case

On July 4 a mixture of dust, marine and continental aerosols was observed at Finokalia station. Figure 11a, shows at 4-6 UTC an advected depolarizing dust plume at 4-6 km and a less-depolarizing plume extending from the ground up to 2-3 km, with volume depolarization ratios at 532 nm of 0.1 and <0.05, respectively. This is a weak dust episode, with a measured column AOD of ~0.15 at 500 nm, which according to the AERONET and GARRLiC uncertainty standards discussed in Section 4.2 should not be sufficient for a full characterization of the particles. The dust and marine particle transport is supported by the BSC DREAM8b dust model and RAMS-ICLAMS sea salt model simulations (Fig. 12b, left), respectively, as well as from our FLEXPART-WRF source-receptor calculations (Fig. 11b). The latter show mainly Saharan dust particles at 4-6 km, marine particles mostly from the Aegean Sea along with continental particles from the Balkans up to 1 km, and a mixture of marine, continental and dust particles at 1-3 km.

GARRLiC retrieves these three layers (Fig. 12a) but it cannot characterize them effectively in terms of their refractive indices, since it is able to retrieve only one refractive index for each mode. For example, the coarse mode of the dust/marine mixture contains dust particles with a real part of refractive index of ~1.55-1.65 (e.g. Kandler et al., 2007) together with marine particles of quite different refractive index, with a real part of ~1.35 (Dubovik et al., 2002). Thus, what we get from GARRLiC as the refractive index of the mixture coarse mode is possibly closer to an average of the refractive indices of dust and marine particles. This is shown in Fig. 13 (down, right), with the GARRLiC coarse mode refractive index to have a value of 1.45 for the real part. The imaginary part of the coarse mode and the SSA show an unusual increase and decrease, respectively, towards the longer wavelengths, which is most probably false. The fine mode should contain mostly continental particles, but the retrieved refractive index of 1.36+i0.001 is more characteristic for marine particles (Dubovik et al., 2002). The AERONET retrieval (used in LIRIC algorithm), assigns a marine refractive index (~1.35+i0.0005) to both fine and coarse particles. The fine mode size distribution compares well with AERONET, but present slightly lower values than SMPS surface in-situ measurements (Fig. 13, up left). With a surface RH of 75%, corresponding to a hygroscopic growth factor of 1.3 (Eq. 2), the GARRLiC fine particle size distribution should be larger than the SMPS dried particle measurements.

Figure 14 shows the potential of GARRLiC to retrieve the "marine" and "dust" components of the mixture, by changing the definition of the two modes retrieved: instead of "fine" and "coarse" mode GARRLiC is set to retrieve two modes that span the whole size range so as both contain coarse particles, and it derives a "dust" mode that contains only coarse particles and a "marine" mode that contains both fine and coarse particles, of bigger size than "dust". Raptis et al. (2015) showed similar results for the marine and dust size distribution using their multimodal analysis for a different dust/marine mixture case during the CHARADMExp campaign. The retrieved real part of the refractive index is ~1.33 for "marine" particles and ~1.47 for "dust" particles. Although these values are very close to the climatological values for marine and dust particles, the retrievals of the imaginary part of the refractive index and the volume concentration profiles are not satisfactory (not shown here). We believe that these results show a potential for successful marine/dust mixture characterization from GARRLiC in the future, if the new versions of the algorithm utilize the cross-polarized signals as well. As in LIRIC, the polarization measurements will help to derive the spherical (marine) and non-spherical (dust) components of the mixture.

LIRIC provides the dust and marine vertical distribution, since it disentangles the coarse particle volume concentration profile to its spherical (marine) and non-spherical (dust) components (Fig. 12a, right). Assuming a very low contribution from dust and marine particles in the fine mode we acquire the "marine" and "dust" concentration profiles from the spherical and non-spherical coarse particle concentration profiles, respectively. The left plot of Fig. 12b shows that LIRIC marine and dust mass concentration profiles have larger values than the BSC DREAM8b dust and the RAMS-ICLAMS sea salt models, respectively. In order to acquire the mass concentration profiles, LIRIC dust and marine volume profiles are multiplied with the density values of $2.6\ \mathrm{g\,cm^{-3}}$ (Reid et al., 2003) and $1.25\ \mathrm{g\,cm^{-3}}$, respectively. The marine particle density corresponds to 60-80% RH (Zhang et al., 2005), as this is provided by the RAMS model at 0-1 km. We believe that BSC DREAM8b model underestimates the dust concentration, as for the dust case in section 4.1, since the model AOD of ~0.025 at 500 nm is approximately 5 times lower than the sun-photometer measured AOD at 550 nm (not taking into account the AOD contribution of the marine and continental particles). Multiplying the BSC DREAM8b dust profile by 5 we get a better agreement with LIRIC dust profile at 4-6 km, but in the mixed layer at 0-3 km this agreement is not satisfactory (not shown here). The RAMS-ICLAMS model show lower sea salt concentration than LIRIC (as in section 4.2), with ~60 %

differences at the surface level. The right plot in Fig. 12b shows that LIRIC PM_{10} values agree well with the surface in situ measurements, within the latter time variability. The LIRIC PM_{10} is calculated using the volume percentage of the particles with diameter less than 10 μm (i.e., 60% of the total volume). Moreover, we calculate the LIRIC "dry" PM_{10} using Eq.1 and considering a particle hygroscopic growth of 1.3 for RH=75% at the surface (Eq.2). The LIRIC "dry" PM_{10} is lower than the surface in situ measurements, at ~50% of their mean value. For GARRLiC the PM_{10} profile cannot be calculated, since the corresponding volume concentration profile is a mixture of dust, marine and continental particles with unknown density.

Figure 15 shows the backscatter and extinction coefficients retrieved with GARRLiC, LIRIC and Klett methods. GARRLiC and LIRIC agree well within the LIRIC uncertainties (Fig. 15, first and second row). The agreement with Klett retrievals is satisfactory for the backscatter coefficient at 532 and 1064 nm above 550 m, within their uncertainties, with 60-130% differences seen for the 355 nm retrieval (Fig. 15, third row). As for the marine case in section 4.2, the NF backscatter coefficient at 532 nm show much larger values. The same holds for the NF extinction coefficient at 532 nm. The Klett extinction coefficients at 1-3 km are up to 60% and 50% lower than GARRLiC at 355 and 532 nm, respectively.

Overall, this is a challenging case for both GARRLiC and LIRIC algorithms. We can claim that GARRLiC shows some potential in providing a successful dust and marine microphysical property characterization in case more information (e.g. cross-polarized lidar signal) is included in the retrieval. Moreover, the LIRIC capability of providing the vertical distribution of dust and marine particles is mostly successful, comparing the results with our source-receptor simulations and the surface in situ PM_{10} measurements. As is the case also for the marine particle characterization in section 4.2, we believe that this retrieval will be greatly benefited from NF measurements.

4 Summary and Conclusions

GARRLiC and LIRIC algorithms provide the great innovation of retrieving the vertical distribution of aerosol microphysics utilizing the synergy of the elastic backscatter lidar and sun-photometer techniques. This way, the algorithms show the potential to effectively characterize the vertical distribution of fine, coarse spherical and coarse non-spherical particle concentrations in the case of LIRIC, and the concentration profiles of fine and coarse particles,

along with their column-averaged size, shape and spectral refractive index, in case of GARRLiC.

In this study we used both algorithms to characterize three cases of dust and marine presence during the ESA-CHARADMExp experimental campaign. For the first case GARRLiC achieves a successful retrieval of the dust vertical distribution and microphysical characterization that agrees well with AERONET and climatological values for dust. Both LIRIC and GARRLiC concentration profiles are found to be consistent with the BSC DREAM8b dust vertical structure, showing though larger values from the surface in situ PM_{10} measurements. For the second case consisting of mainly marine particles, both algorithms provide satisfactory concentration retrievals comparing with the surface in situ PM_{10} measurements. The GARRLiC microphysical property retrieval is mostly not successful for the marine particles. This is due to the difficulties posed by the really low AOD and the insufficient lidar information in the overlap region, where most of the marine aerosol load resides. Last, for the more challenging case of dust and marine mixture, LIRIC provides the dust and marine particle vertical structure due to its capability to retrieve the coarse mode spherical (marine) and non-spherical (dust) components. GARRLiC shows potential in disentangling the marine and dust components, if more information is included in the algorithm input.

The difficulties posed in retrieving the concentration profiles and the microphysical properties of dust and marine particle mixtures in the atmospheric column have to do with the low AOD of the marine plumes, the insufficient lidar information in the overlap region and the number of modes considered from the retrievals. For GARRLiC, the retrieval of multiple modes would be possibly feasible in the future with the incorporation of polarimetric measurements from the sun-photometer and/or the cross-polarized and Raman signals from the lidar. Moreover, we could try to increase the near-to-surface information from the lidar, performing the signal gluing technique between the FF and NF measurements. We aim to continue investigating the GARRLiC and LIRIC potential for aerosol characterization and follow related improvements in the framework of the ACTRIS-2 project and the experimental campaigns that are dedicated to that objective.

Acknowledgements

The research leading to these results has received funding from the European Union's Horizon 2020 Research and Innovation Programme ACTRIS-2 (grant agreement no. 654109). The work has been developed under the auspices of the ESA-ESTEC project "Characterization of Aerosol mixtures of Dust And Marine origin" contract no. IPL-PSO/FF/lf/14.489. The publication was supported by the European Union's Horizon 2020 Research and Innovation programme under grant agreement No 602014, project ECARS (East European Centre for Atmospheric Remote Sensing). BSC-DREAM8b simulations were performed on the Mare Nostrum supercomputer hosted by the Barcelona Supercomputing Center–Centro Nacional de Supercomputación (BSC).

References

Althausen, D., Engelmann, R., Baars, H., Heese, B., Ansmann, A., Mueller, D., and Komppula, M.: Portable Raman lidar PollyXT for automated profiling of aerosol backscatter, extinction, and depolarization, Journal of Atmospheric and Oceanic Technology, 26, 2366–2378, 10.1175/2009JTECHA1304.1, 2009.

Amiridis, V., Kafatos, M., Pérez, C., Kazadzis, S., Gerasopoulos, E., Mamouri, R. E., Papayannis, A., Kokkalis, P., Giannakaki, E., Basart, S., Daglis, I., and Zerefos, C.: The potential of the synergistic use of passive and active remote sensing measurements for the validation of a regional dust model, Ann. Geophys., 27, 3155–3164, doi:10.5194/angeo-27-3155-2009, 2009.

Amiridis, V., Wandinger, U., Marinou, E., Giannakaki, E., Tsekeri, A., Basart, S., Kazadzis, S., Gkikas, A., Taylor, M., Baldasano, J., and Ansmann, A.: Optimizing Saharan dust CALIPSO retrievals, Atmos. Chem. Phys. Discuss., 13, 14749–14795, doi:10.5194/acpd-13-14749-2013, 2013.

Ansmann, A., Riebesell, M., and Weitkamp, C.: Measurement of atmospheric aerosol extinction profiles with a Raman lidar, Opt. Lett., 15, 746-748, 1990.

Ansmann, A., Tesche, M., Seifert, P., Groß, S., Freudenthaler, V., Apituley, A., Wilson, K. M., Serikov, I., Linné, H., Heinold, B., Hiebsch, A., Schnell, F., Schmidt, J., Mattis, I., Wandinger, U., and Wiegner, M.: Ash and fine-mode particle mass profiles from EARLINET-AERONET observations over central Europe after the eruptions of the Eyjafjallajökull volcano in 2010, J. Geophys. Res. Atmospheres, 116(D20), D00U02, doi:10.1029/2010JD015567, 2011.

Ansmann, A., Seifert, P., Tesche, M., and Wandinger, U.: Profiling of fine and coarse particle mass: case studies of Saharan dust and Eyjafjallajökull/Grimsvötn volcanic plumes, Atmos Chem Phys, 12(20), 9399–9415, doi:10.5194/acp-12-9399-2012, 2012.

Baars, H., Kanitz, T., Engelmann, R., Althausen, D., Heese, B., Komppula, M., Preißler, J., Tesche, M., Ansmann, A., Wandinger, U., Lim, J.-H., Ahn, J. Y., Stachlewska, I. S., Amiridis, V., Marinou, E., Seifert, P., Hofer, J., Skupin, A., Schneider, F., Bohlmann, S., Foth, A., Bley, S., Pfüller, A., Giannakaki, E., Lihavainen, H., Viisanen, Y., Hooda, R. K., Pereira, S. N., Bortoli, D., Wagner, F., Mattis, I., Janicka, L., Markowicz, K. M., Achtert, P., Artaxo, P., Pauliquevis, T., Souza, R. A. F., Sharma, V. P., van Zyl, P. G., Beukes, J. P., Sun, J., Rohwer, E. G., Deng, R., Mamouri, R.-E., and Zamorano, F.: An overview of the first decade of Polly^{NET}:

an emerging network of automated Raman-polarization lidars for continuous aerosol profiling, Atmos. Chem. Phys., 16, 5111-5137, doi:10.5194/acp-16-5111-2016, 2016.

Balis, D., Amiridis, V., Nickovic, S., Papayannis, A., and Zerefos, C.: Optical properties of Saharan dust layers as detected by a Raman lidar at Thessaloniki, Greece, Geophysical Research Letters, 31, L13104, doi:10.1029/2004GL019881, 2004.

Basart, S., Pérez García-Pando, C., Cuevas, E., Baldasano Recio, J. M., and Gobbi, P.: Aerosol characterization in Northern Africa, Northeastern Atlantic, Mediterranean basin and Middle East from direct-sun AERONET observations, Atmospheric Chemistry and Physics, 9(21), 8265-8282, 2009.

Basart, S., Pérez, C., Nickovic, S., Cuevas, E., and Baldasano, J. M.: Development and evaluation of the BSC-DREAM8b dust regional model over Northern Africa, the Mediterranean and the Middle East, Tellus B, 64, 18539, doi:10.3402/tellusb.v64i0.18539, 2012a.

Basart, S., Pay, M. T., Jorba, O., Pérez, C., Jiménez-Guerrero, P., Schulz, M., and Baldasano, J. M.: Aerosols in the CALIOPE air quality modelling system: evaluation and analysis of PM levels, optical depths and chemical composition over Europe, Atmos. Chem. Phys., 12, 3363–3392, doi:10.5194/acp-12-3363-2012, 2012b.

Binietoglou, I., Basart, S., Alados-Arboledas, L., Amiridis, V., Argyrouli, A., Baars, H., Baldasano, J. M., Balis, D., Belegante, L., Bravo-Aranda, J. A., Burlizzi, P., Carrasco, V., Chaikovsky, A., Comerón, A., D'Amico, G., Filioglou, M., Granados-Muñoz, M. J., Guerrero-Rascado, J. L., Ilic, L., Kokkalis, P., Maurizi, A., Mona, L., Monti, F., Muñoz-Porcar, C., Nicolae, D., Papayannis, A., Pappalardo, G., Pejanovic, G., Pereira, S. N., Perrone, M. R., Pietruczuk, A., Posyniak, M., Rocadenbosch, F., Rodríguez-Gómez, A., Sicard, M., Siomos, N., Szkop, A., Terradellas, E., Tsekeri, A., Vukovic, A., Wandinger, U., and Wagner, J.: A methodology for investigating dust model performance using synergistic EARLINET/AERONET dust concentration retrievals, Atmos. Meas. Tech., 8, 3577-3600, doi:10.5194/amt-8-3577-2015, 2015.

Bezantakos, S., Barmpounis, K., Giamarelou, M., Bossioli, E., Tombrou, M., Mihalopoulos, N., Eleftheriadis, K., Kalogiros, J., D. Allan, J., Bacak, A., Percival, C. J., Coe, H., and Biskos, G.: Chemical composition and hygroscopic properties of aerosol particles over the Aegean Sea, Atmos. Chem. Phys., 13, 11595-11608, doi:10.5194/acp-13-11595-2013, 2013.

Bovchaliuk, V., Goloub, P., Podvin, T., Veselovskii, I., Tanre, D., Chaikovsky, A., Dubovik, O., Mortier, A., Lopatin, A., Korenskiy, M., and Victori, S.: Comparison of aerosol properties retrieved using GARRLiC, LIRIC, and Raman algorithms applied to multi-wavelength LIDAR and sun/sky-photometer data, Atmos. Meas. Tech. Discuss., doi:10.5194/amt-2016-40, in review, 2016.

Brioude, J., Arnold, D., Stohl, A., Cassiani, M., Morton, D., Seibert, P., Angevine, W., Evan, S., Dingwell, A., Fast, J. D., Easter, R. C., Pisso, I., Burkhart, J., and Wotawa, G.: The Lagrangian particle dispersion model FLEXPART-WRF version 3.1, Geosci. Model Dev., 6, 1889-1904, doi:10.5194/gmd-6-1889-2013, 2013.

Chaikovsky, A., Dubovik, O., Holben, B., Bril, A., Goloub, P., Tanré, D., Pappalardo, G., Wandinger, U., Chaikovskaya, L., Denisov, S., Grudo, J., Lopatin, A., Karol, Y., Lapyonok, T., Amiridis, V., Ansmann, A., Apituley, A., Allados-Arboledas, L., Binietoglou, I., Boselli, A., D'Amico, G., Freudenthaler, V., Giles, D., Granados-Muñoz, M. J., Kokkalis, P., Nicolae, D., Oshchepkov, S., Papayannis, A., Perrone, M. R., Pietruczuk, A., Rocadenbosch, F., Sicard, M., Slutsker, I., Talianu, C., De Tomasi, F., Tsekeri, A., Wagner, J., and Wang, X.: Lidar-Radiometer Inversion Code (LIRIC) for the retrieval of vertical aerosol properties from combined lidar/radiometer data: development and distribution in EARLINET, Atmos. Meas. Tech., 9, 1181-1205, doi:10.5194/amt-9-1181-2016, 2016.

Cotton, W. R., Pielke, Sr., R. A., Walko, R. L., Liston, G. E., Tremback, C. J., Jiang, H., McAnelly, R. L., Harrington, J. Y., Nicholls, M. E., Carrio, G. G., and Mc Fadden, J. P.: RAMS 2001: Current status and future directions, Meteorol. Atmos. Phys., 82, 5–29, 2003.

Dubovik, O. and King, M: A flexible inversion algorithm for retrieval of aerosol optical properties from Sun and sky radiance measurements, J. Geophys. Res., 105, 20673–20696, doi:10.1029/2000JD900282, 2000a.

Dubovik, O., Smirnov, A., Holben, B. N., King, M. D., Y. J. Kaufman, Eck, T. F., and Slutsker, I.: Accuracy assessment of aerosol optical properties retrieval from AERONET sun and sky radiance measurements, J. Geophys. Res., 105, 9791–9806, 2000b.

Dubovik, O., Holben, B., Eck, T., Smirnov, A., Kaufman, Y., King, M., Tanré, D., and Slutsker, I.: Variability of absorption and optical properties of key aerosol types observed in worldwide locations, J. Atmos. Sci., 59, 590–608, 2002.

Dubovik, O.: Optimization of Numerical Inversion in Photopolarimetric Remote Sensing, in: Photopolarimetry in Remote Sensing, edited by: Videen, G., Yatskiv, Y., and Mishchenko, M., Kluwer Academic Publishers, Dordrecht, the Netherlands, 65–106, 2004.

Dubovik, O., Sinyuk, A., Lapyonok, T., Holben, B. N., Mishchenko, M., Yang, P., Eck, T.F., Volten, H., Muñoz, O., Veihelmann, B., van der Zande, W. J., Leon, J. -F., Sorokin, M., and Slutsker, I.: Application of spheroid models to account for aerosol particle nonsphericity in remote sensing of desert dust, J. Geophys. Res., 111, D11208, doi:10.1029/2005JD006619, 2006.

Dubovik, O., Lapyonok, T., Litvinov, P., Herman, M., Fuertes, D., Ducos, F., Lopatin, A., Chaikovsky, A., Torres, B., Derimian, Y., Huang, X., Aspetsberger, M., and Federspiel, C.: GRASP: a versatile algorithm for characterizing the atmosphere, SPIE: Newsroom, Sep., 2014.

Engelmann, R., Kanitz, T., Baars, H., Heese, B., Althausen, D., Skupin, A., Wandinger, U., Komppula, M., Stachlewska, I. S., Amiridis, V., Marinou, E., Mattis, I., Linné, H., and Ansmann, A.: The automated multiwavelength Raman polarization and water-vapor lidar Polly^{XT}: the neXT generation, Atmos. Meas. Tech., 9, 1767-1784, doi:10.5194/amt-9-1767-2016, 2016.

Fernald, F. G., Herman, B. M., and Reagan, J. A.: Determination of aerosol height distributions by lidar, J. Appl. Meteorol., 11, 482–489, 1972.

Gerasopoulos E., Kouvarakis G., Babasakalis P., Vrekoussis M., Putaud J.P., and Mihalopoulos N.: Origin and variability of particulate matter (PM10) mass concentrations over the Eastern Mediterranean, Atmos. Environ., 40, 4679-4690, 2006.

Gobbi, G. P., Angelini, F., Barnaba, F., Costabile, F., Baldasano, J. M., Basart, S., and Bolignano, A.: Changes in particulate matter physical properties during Saharan advections over Rome (Italy): a four-year study, 2001–2004. Atmospheric Chemistry and Physics, 13(15), 7395-7404, 2013.

Gong, S. L., Barrie, L. A., and Lazare, M.: Canadian Aerosol Module (CAM): a size-segregated simulation of atmospheric aerosol processes for climate and air quality models. 2. Global sea-salt aerosol and its budgets, J. Geophys. Res., 107(D24), 4779, doi:10.1029/2001JD002004, 2002.

Granados-Muñoz, M. J., Guerrero-Rascado, J. L., Bravo-Aranda, J. A., Navas-Guzmán, F., Valenzuela, A., Lyamani, H., Chaikovsky, A., Wandinger, U., Ansmann, A., Dubovik, O., Grudo, J., and Alados-Arboledas, L.: Retrieving aerosol microphysical properties by Lidar-Radiometer Inversion Code (LIRIC) for different aerosol types, J. Geophys. Res., 119, 4836–4858, doi:10.1002/2013JD021116, 2014.

Granados-Muñoz, M. J., Bravo-Aranda, J. A., Baumgardner, D., Guerrero-Rascado, J. L., Pérez-Ramírez, D., Navas-Guzmán, F., Veselovskii, I., Lyamani, H., Valenzuela, A., Olmo, F. J., Titos, G., Andrey, J., Chaikovsky, A., Dubovik, O., Gil-Ojeda, M., and Alados-Arboledas, L.: Study of aerosol microphysical properties profiles retrieved from ground-based remote sensing and aircraft in-situ measurements during a Saharan dust event, Atmos. Meas. Tech. Discuss., 8, 9289–9338, doi:10.5194/amtd-8-9289-2015, 2015.

Granados-Muñoz, M. J., Navas-Guzmán, F., Guerrero-Rascado, J. L., Bravo-Aranda, J. A., Binietoglou, I., Pereira, S. N., Basart, S., Baldasano, J. M., Belegante, L., Chaikovsky, A., Comerón, A., D'Amico, G., Dubovik, O., Ilic, L., Kokkalis, P., Muñoz-Porcar, C., Nickovic, S., Nicolae, D., Olmo, F. J., Papayannis, A., Pappalardo, G., Rodríguez, A., Schepanski, K., Sicard, M., Vukovic, A., Wandinger, U., Dulac, F., and Alados-Arboledas, L.: Profiling of aerosol microphysical properties at several EARLINET/AERONET sites during the July 2012 ChArMEx/EMEP campaign, Atmos. Chem. Phys., 16, 7043-7066, doi:10.5194/acp-16-7043-2016, 2016.

Haustein, K., Pérez, C., Baldasano, J. M., Müller, D., Tesche, M., Schladitz, A., Freudenthaler, V., Heese, B., Esselborn, M., Weinzierl, B., Kandler, K., and von Hoyningen-Huene, W.: Regional dust model performance during SAMUM 2006, Geophys. Res. Lett., 36, L03812, doi:10.1029/2008GL036463, 2009.

Ho, S. -p., Peng, L., Anthes, R. A., Kuo, Y. -H., and Lin, H. -C.: Marine Boundary Layer Heights and Their Longitudinal, Diurnal, and Interseasonal Variability in the Southeastern Pacific Using COSMIC, CALIOP, and Radiosonde Data, Journal of Climate, 28, 2856, 2015.

Holben, B. N., Eck, T. F., Slutsker, I., Tanre, D., Buis, J. P., Setzer, A., Vermote, E., Reagan, J. A., Kaufman, Y. J., Nakajima, T., Lavenu, F., Jankowiak, I., and Smirnov, A.: AERONET-A federated instrument network and data archive for aerosol characterization, Remote Sens. Environ., 66(1), 1–16, doi:10.1016/S0034-4257(98)00031-5, 1998.

Jiménez-Guerrero, P., Pérez, C., Jorba, O., and Baldasano, J. M.: Contribution of Saharan dust in an integrated air quality system and its on-line assessment, Geophys. Res. Lett., 35, L03814, doi:10.1029/2007GL031580, 2008.

Kalivitis, N., Gerasopoulos, E., Vrekoussis, M., Kouvarakis, G., Kubilay, N., Hatzianastassiou, N., Vardavas, I., and Mihalopoulos, N.: Dust transport over the eastern Mediterranean derived from Total Ozone Mapping Spectrometer, Aerosol Robotic Network, and surface measurements, J. Geophys. Res., 112, D03202, doi:10.1029/2006JD007510, 2007.

Klett, D.: Lidar inversion with variable backscatter/extinction ratios, Appl. Optics, 31, 1638–1643, 1985.

Kokkalis, P., Amiridis, V., Allan, J. D., Papayannis, A., Solomos, S., Tsekeri, A., Rosenberg, P. D., Binietoglou, I., Marinou, E., Vasilescu, J., Nicolae, D., Coe, H., Bacak, A., Chaikovsky, A.: Validation of LIRIC aerosol concentration retrievals using airborne measurements over Athens, submitted in Atmospheric Research, 2016.

Lawrence, M.G.: The relationship between relative humidity and the dewpoint temperature in moist air: a simple conversion and applications, Bull. Am. Meteorol. Soc., 86, 225–233, 2005, http://dx.doi.org/10.1175/BAMS-86-2-225.

Leeuw, G., Neele, F. P., Hill, M., Smith, M. H., and Vignali, E.: Production of sea spray aerosol in the surf zone, J. Geophys. Res. Atmos., 105, 29397–29409, 2000.

Lelieveld, J., Berresheim, H., Borrmann, S., Crutzen, P., Dentener, F., Fischer, H., Feichter, J., Flatau, P., Heland, J., Holzinger, R., Korrmann, R., Lawrence, M., Levin, Z., Markowicz, K., Mihalopoulos, N., Minikin, A., Ramanathan, V., de Reus, M., Roelofs, G., Scheeren, H., Sciare, J., Schlager, H., Schultz, M., Siegmund, P., Steil, B., Stephanou, E., Stier, P., Traub, M., Warneke, C., Williams, J., and Ziereis, H.: Global air pollution crossroads over the Mediterranean, Science, 298, 794–799, doi: 10.1126/science.1075457, 2002.

Lopatin, A., Dubovik, O., Chaikovsky, A., Goloub, P., Lapyonok, T., Tanré, D., and Litvinov, P.: Enhancement of aerosol characterization using synergy of lidar and sun-photometer coincident observations: the GARRLiC algorithm, Atmos. Meas. Tech., 6, 2065-2088, doi:10.5194/amt-6-2065-2013, 2013.

Ming, Y., and L. M. Russell: Predicted hygroscopic growth of sea salt aerosol, J. Geophys. Res., 106(D22), 28259–28274, doi:10.1029/2001JD000454, 2001.

Mona, L., Amodeo, A., D'Amico, G., Giunta, A., Madonna, F., and Pappalardo, G.: Multi-wavelength Raman lidar observations of the Eyjafjallajökull volcanic cloud over Potenza, southern Italy, Atmos. Chem. Phys., 12, 2229–2244, doi:10.5194/acp-12-2229-2012, 2012.

Mona, L., Papagiannopoulos, N., Basart Alpuente, S., Baldasano Recio, J. M., Binietoglou, I., Cornacchia, C., & Pappalardo, G.: EARLINET dust observations vs. BSC-DREAM8b modeled profiles: 12-year-long systematic comparison at Potenza, Italy. Atmospheric chemistry and physics, 14(16), 8781-8793, 2014.

Monahan, E. C., Spiel, D. E., and Davidson, K. L.: A model of marine aerosol generation via whitecaps and wave disruption, in: Oceanic Whitecaps, edited by: Monahan, E. C. and Mac Niocaill, G., Reidel, D., 167–174, 1986.

Mishra, A. K., Klingmueller, K., Fredj, E., Lelieveld, J., Rudich, Y., and Koren, I.: Radiative signature of absorbing aerosol over the eastern Mediterranean basin, Atmos. Chem. Phys., 14, 7213-7231, doi:10.5194/acp-14-7213-2014, 2014.

Müller, D., Böckmann, C., Kolgotin, A., Schneidenbach, L., Chemyakin, E., Rosemann, J., Znak, P., and Romanov, A.: Microphysical particle properties derived from inversion algorithms developed in the framework of EARLINET, Atmos. Meas. Tech. Discuss., 8, 12823-12885, doi:10.5194/amtd-8-12823-2015, 2015.

Nickovic, S., Kallos, G., Papadopoulos, A., and Kakaliagou, O.: A model for prediction of desert dust cycle in the atmosphere, J. Geophys. Res., 106, 18113–18130, doi:10.1029/2000JD900794, 2001.

Otto, S., de Reus, M., Trautmann, T., Thomas, A., Wendisch, M., and Borrmann, S.: Atmospheric radiative effects of an in situ measured Saharan dust plume and the role of large particles, Atmos. Chem. Phys., 7, 4887-4903, doi:10.5194/acp-7-4887-2007, 2007.

Papayannis, A., Balis, D., Amiridis, V., Chourdakis, G., Tsaknakis, G., Zerefos, C., Castanho, A. D. A., Nickovic, S., Kazadzis, S., and Grabowski, J.: Measurements of Saharan dust aerosols over the Eastern Mediterranean using elastic backscatter-Raman lidar, spectrophotometric and satellite observations in the frame of the EARLINET project, Atmos. Chem. Phys., 5, 2065-2079, doi:10.5194/acp-5-2065-2005, 2005.

Papayannis, A., Nicolae, D., Kokkalis, P., Binetoglou, I., Talianu, C., Belegante, L., Tsaknakis., G., Cazacu, M. M., Vetres, I., and Ilic, I.: Optical, size and mass properties of mixed type

aerosols in Greece and Romania as observed by synergy of lidar and sunphotometers in combination with model simulations: A case study, Sci. Tot. Environ., 500–501, 277–294, 2014.

Pappalardo, G., Amodeo, A., Apituley, A., Comeron, A., Freudenthaler, V., Linné, H., Ansmann, A., Bösenberg, J., D'Amico, G., Mattis, I., Mona, L., Wandinger, U., Amiridis, V., Alados Arboledas, L., Nicolae, D., and Wiegner, M.: EARLINET: towards an advanced sustainable European aerosol lidar network, Atmos. Meas. Tech., 7, 2389–2409, doi:10.5194/amt-7-2389-2014, 2014.

Pay, M. T., Piot, M., Jorba, O., Gassó, S., Gonçalves, M., Basart, S., Dabdub, D., Jiménez-Guerrero, P., and Baldasano, J. M.: A full year evaluation of the CALIOPE-EU air quality modeling system over Europe for 2004, Atmos. Environ., 44, 3322–3342, doi:10.1016/j.atmosenv.2010.05.040, 2010.

Pay, M. T., Jiménez-Guerrero, P., Jorba, O., Basart, S., Querol, X., Pandolfi, M., and Baldasano, J. M.: Spatio-temporal variability of concentrations and speciation of particulate matter across Spain in the CALIOPE modeling system, Atmos. Environ., 46, 376–396, 2012.

Pérez, C., Nickovic, S., Pejanovic, G., Baldasano, J. M., and Ozsoy, E.: Interactive dust-radiation modeling: a step to improve weather forecasts, J. Geophys. Res., 11, D16206, doi:10.1029/2005JD006717, 2006a.

Pérez, C., Nickovic, S., Baldasano, J. M., Sicard, M., Rocadenbosch, F., and Cachorro, V. E.: A long Saharan dust event over the western Mediterranean: lidar, sun photometer observations, and regional dust modeling, J. Geophys. Res., 111, D15214, doi:10.1029/2005JD006579, 2006b.

Petters, M. D. and Kreidenweis, S. M.: A single parameter representation of hygroscopic growth and cloud condensation nucleus activity, Atmos. Chem. Phys., 7, 1961–1971, doi:10.5194/acp-7-1961-2007, 2007.

Pielke, R. A., Cotton, W. R., Walko, R. L., Tremback, C. J., Lyons, W. A., Grasso, L. D., Nicholls, M. E., Moran, M. D., Wesley, D. A., Lee, T. J., and Copeland, J. H.: A comprehensive meteorological modeling system—RAMS, Meteor. Atmos. Phys., 49, 69–91, 1992.

Prospero, J. M.: Saharan dust transport over the North Atlantic Ocean and Mediterranean: an overview, in: The Impact of Desert Dust Across the Mediterranean (eds. S. Guerzoni and R. Chester), Kluwer Academic, Dordrecht, pp. 133–151, 1996.

Raptis, P. I., Kokkalis, P., Amiridis, V., Taylor, M. and Kazadzis, S.: A case study of columnar marine and dust particle ratios calculated with photometric and lidar measurements during the CHARADMEXP campaign, EGU General Assembly Conference Abstracts, 17, p. 8942, 2015.

Reid, J. S., Jonsson, H. H., Maring, H. B., Smirnov, A., Savoie, D. L., Cliff, S. S., Reid, E. A., Livingston, J. M., Meier, M. M., Dubovik, O., et al: Comparison of size and morphological measurements of coarse mode dust particles from Africa. J. Geophys. Res. Atmos. 2003, 108, doi:10.1029/2002JD002485, 2003.

Sciare J., Oikonomou, K., Favez, O., Markaki, Z., Liakakou, E., Cachier, H., and Mihalopoulos, N.: Long-term measurements of carbonaceous aerosols in the Eastern Mediterranean: Evidence of long-range transport of biomass burning, Atmos. Chem. Phys., 8, 5551-5563, 2008.

Seinfeld, J. H. and Pandis, S. N.: Atmospheric Chemistry and Physics: From Air Pollution to Climate Change, J. Wiley, Sons, Inc., New York, 1998.

Siomos, N., Balis, D. S., Poupkou, A., Liora, N., Dimopoulos, S., Melas, D., Giannakaki, E., Filioglou, M., Basart, S., and Chaikovsky, A.: Investigating the quality of modeled aerosol profiles based on combined lidar and sunphotometer data, Atmos. Chem. Phys., 17, 7003-7023, https://doi.org/10.5194/acp-17-7003-2017, 2017.

Skamarock, W., Klemp, J. B., Dudhia, J., Gill, D. O., Barker, D., Duda, M. G., Huang, X. -Y., and Wang., W.: A description of the Advanced Research WRF version 3, NCAR Technical Note NCAR/TN-475+STR, DOI: 10.5065/D68S4MVH, 2008.

Snider, J. R. and Petters, M. D.: Optical particle counter measurement of marine aerosol hygroscopic growth, Atmos. Chem. Phys., 8, 1949–1962, doi:10.5194/acp-8-1949-2008, 2008.

Solomos, S., Kallos, G., Kushta, J., Astitha, M., Tremback, C., Nenes, A., and Levin, Z.: An integrated modeling study on the effects of mineral dust and sea salt particles on clouds and precipitation, Atmos. Chem. Phys., 11, 873-892, doi:10.5194/acp-11-873-2011, 2011.

Solomon, S., et al.: Intergovernmental Panel on Climate Change, Climate Change 2007: The Physical Science Basis. Contribution of Working Group I to the Fourth Assessment Report of

the Intergovernmental Panel on Climate Change, Cambridge Univ Press, Cambridge, UK, 2007.

Stock, M., Cheng, Y. F., Birmili, W., Massling, A., Wehner, B., Müller, T., Leinert, S., Kalivitis, N., Mihalopoulos, N., and Wiedensohler, A.: Hygroscopic properties of atmospheric aerosol particles over the Eastern Mediterranean: implications for regional direct radiative forcing under clean and polluted conditions, Atmos. Chem. Phys., 11, 4251-4271, doi:10.5194/acp-11-4251-2011, 2011.

Tang, I.N., Tridico, A.C., and Fung, K. H.: Thermodynamic and optical properties of sea salt aerosols, J. Geophys. Res., 102(D19), 23269–23275, doi:10.1029/97JD01806, 1997.

Todd, M. C., Bou Karam, D., Cavazos, C., Bouet, C., Heinold, B., Baldasano, J. M., Cautenet, G., Koren, I., Perez, C., Solmon, F., Tegen, I., Tulet, P., Washington, R., and Zakey, A.: Quantifying uncertainty in estimates of mineral dust flux: an intercomparison of model performance over the Bodélé Depression, northern Chad, J. Geophys. Res., 113, D24107, doi:10.1029/2008JD010476, 2008.

Tsekeri, A., Amiridis, V., Kokkalis, P., Basart, S., Chaikovsky, A., Dubovik, O., Mamouri, R. E., Papayannis, A., and Baldasano, J. M.: Application of a Synergetic Lidar and Sunphotometer Algorithm for the Characterization of a Dust Event Over Athens, Greece, British J. of Environment and Climate Change, 3, 531–546, doi:10.9734/BJECC/2013/2615, 2013.

Tsekeri, A., Amiridis, V., Marenco, F., Nenes, A., Marinou, E., Solomos, S., Rosenberg, P., Trembath, J., Nott, G. J., Allan, J., Le Breton, M., Bacak, A., Coe, H., Percival, C., and Mihalopoulos, N.: Profiling aerosol optical, microphysical and hygroscopic properties in ambient conditions by combining in situ and remote sensing, Atmos. Meas. Tech., 10, 83-107, doi:10.5194/amt-10-83-2017, 2017.

Veselovskii, I., Goloub, P., Podvin, T., Bovchaliuk, V., Derimian, Y., Augustin, P., Fourmentin, M., Tanre, D., Korenskiy, M., Whiteman, D. N., Diallo, A., Ndiaye, T., Kolgotin, A., and Dubovik, O.: Retrieval of optical and physical properties of African dust from multiwavelength Raman lidar measurements during the SHADOW campaign in Senegal, Atmos. Chem. Phys., 16, 7013-7028, doi:10.5194/acp-16-7013-2016, 2016.

Vrekoussis M., Liakakou, E., Koçak, M., Kubilay, N., Oikonomou, K., Sciare J., and Mihalopoulos, N.: Seasonal variability of optical properties of aerosols in the Eastern Mediterranean, Atmos. Environ., 39, 7083-7094, 2005.

Wagner, J., Ansmann, A., Wandinger, U., Seifert, P., Schwarz, A., Tesche, M., Chaikovsky, A., and Dubovik, O.: Evaluation of the Lidar/Radiometer Inversion Code (LIRIC) to determine microphysical properties of volcanic and desert dust, Atmos. Meas. Tech., 6, 1707–1724, doi:10.5194/amt-6-1707-2013, 2013.

Wandinger U. and Ansmann A.: Experimental determination of the lidar overlap profile with Raman lidar, Appl. Opt. 41, 511-514, 2002.

Zhang, K. M., Knipping, E. M., Wexler, A. S., Bhave, P. V., and Tonnesen, G. S.: Size distribution of sea-salt emissions as a function of relative humidity, Atmos. Environ., 39, 3373-3379, 2005.

Atmos. Meas. Tech. Discuss., https://doi.org/10.5194/amt-2017-214
Manuscript under review for journal Atmos. Meas. Tech.
Discussion started: 17 July 2017

Atmospheric Measurement Techniques Discussions

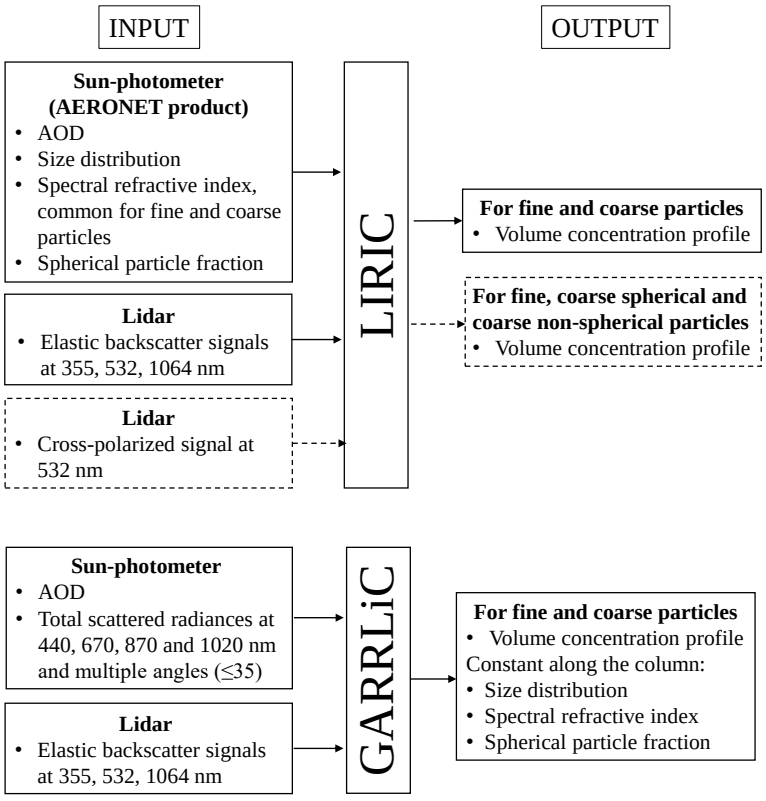

1

2

3 Figure 1. GARRLiC and LIRIC algorithm input and output parameters. For LIRIC, the output
4 in case of using the cross-polarized signal at 532 nm is shown in the dashed box.

Atmos. Meas. Tech. Discuss., https://doi.org/10.5194/amt-2017-214
Manuscript under review for journal Atmos. Meas. Tech.
Discussion started: 17 July 2017

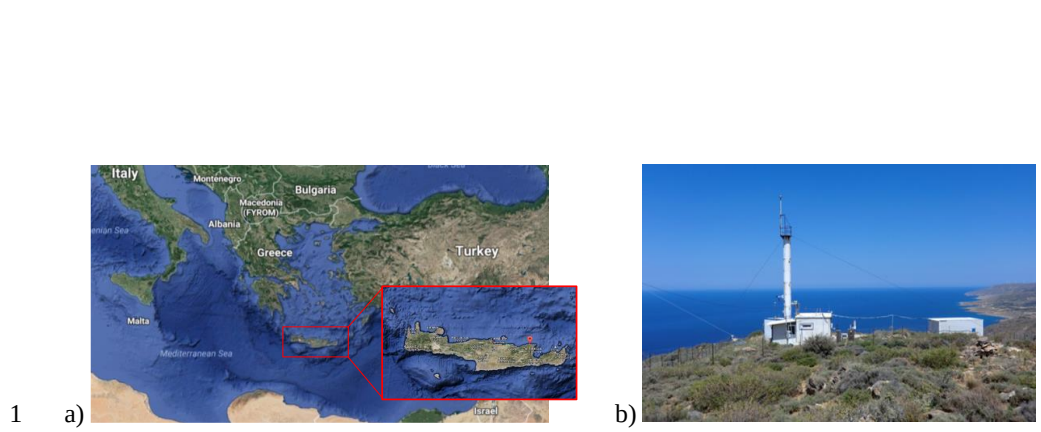

Figure 2. a) Location of Finokalia station (red dot) in Crete island, Greece. b) Sea view from the station.

Atmos. Meas. Tech. Discuss., https://doi.org/10.5194/amt-2017-214
Manuscript under review for journal Atmos. Meas. Tech.
Discussion started: 17 July 2017

Atmospheric Measurement Techniques Discussions

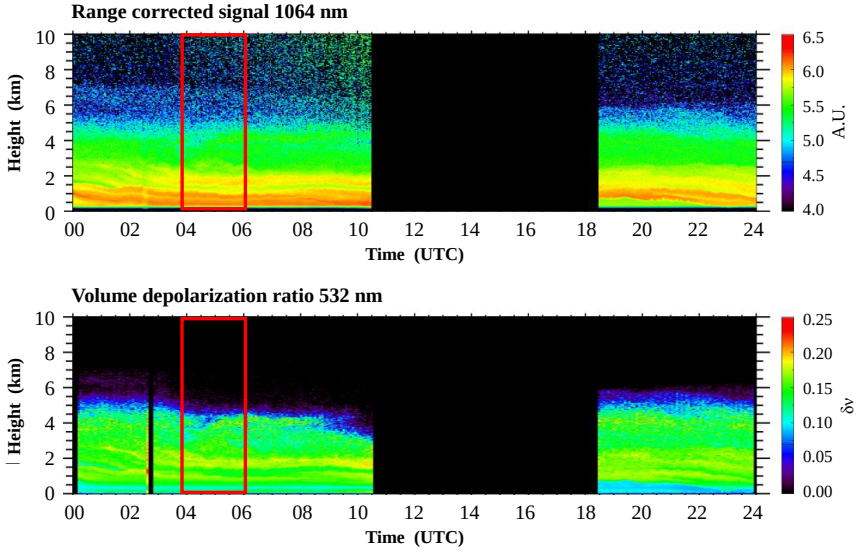

a)

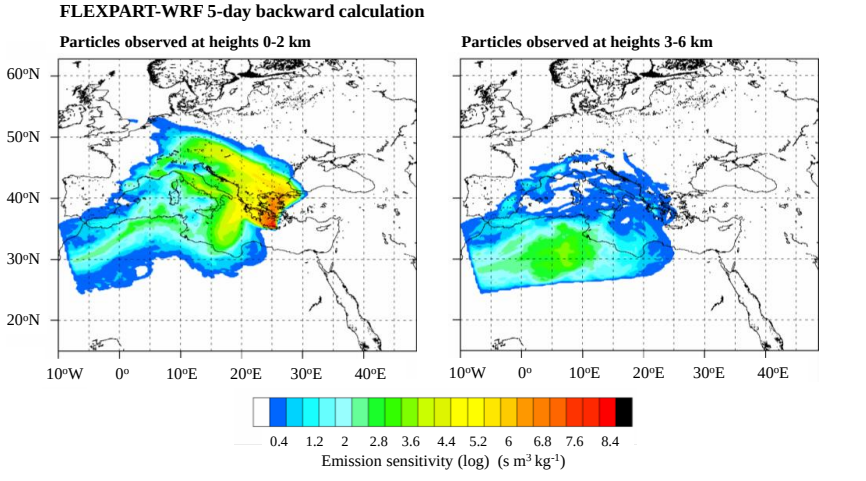

b)

Figure 3. a) Range-corrected backscattered signal at 1064 nm in arbitrary units (top) and volume depolarization ratio at 532 nm (bottom) from Polly^{XT} OCEANET lidar, at Finokalia, Crete, on June 26, 2014. The red rectangle indicates the time range of the measurements used for GARRLiC and LIRIC retrievals (04:00-06:00 UTC). b) Five day backward FLEXPART-WRF calculation of emission sensitivity (i.e., residence time in the lowest 1 km in the atmosphere) in log(s m^3 kg^{-1}) for the particles arriving at 0-2 km (left) and 3-6 km (right) at 04:00 UTC.

Atmos. Meas. Tech. Discuss., https://doi.org/10.5194/amt-2017-214
Manuscript under review for journal Atmos. Meas. Tech.
Discussion started: 17 July 2017

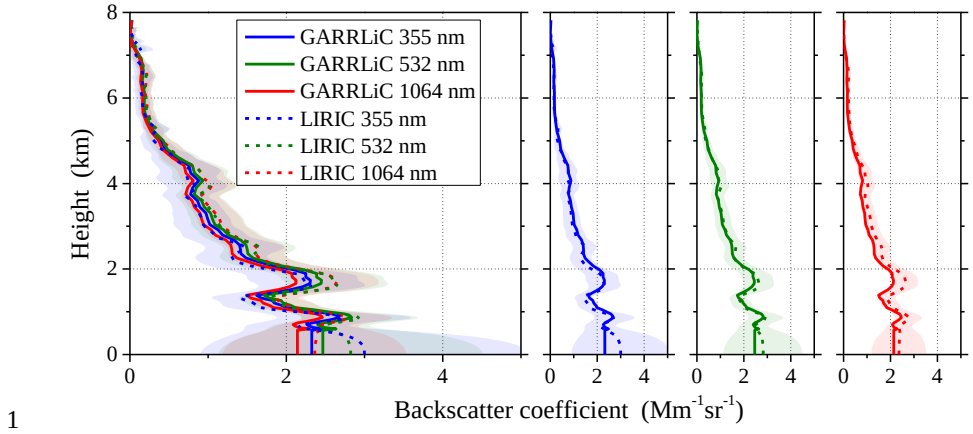

1

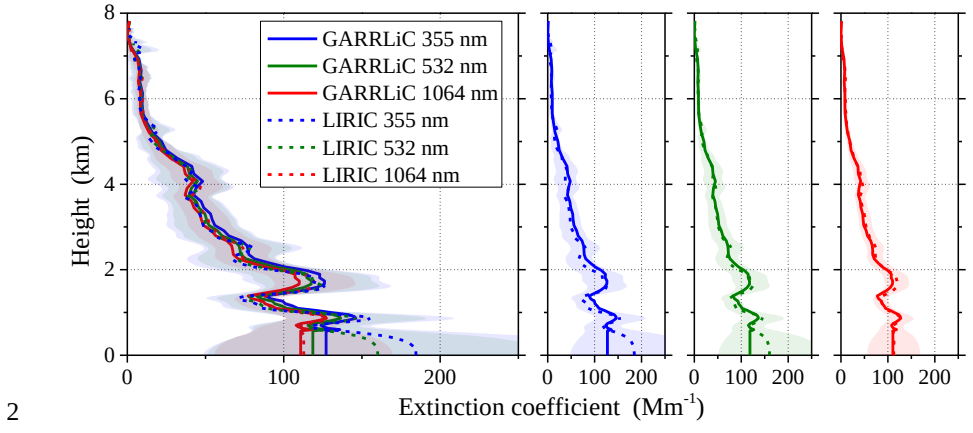

2

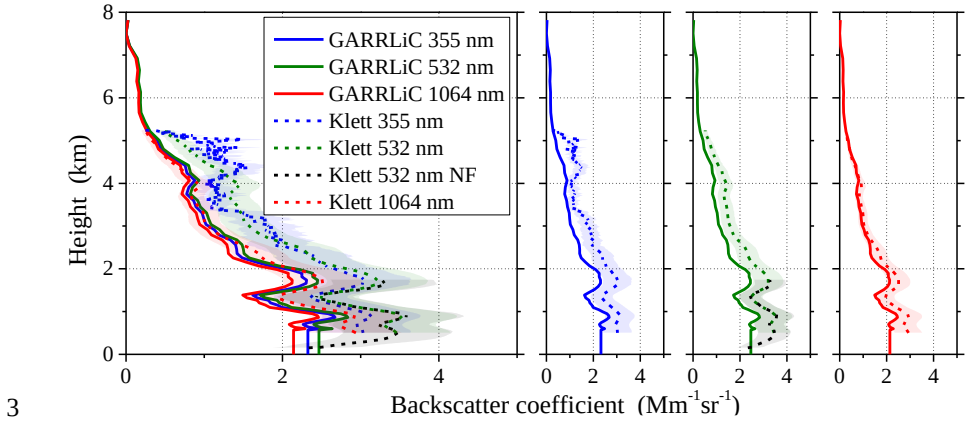

3

Atmos. Meas. Tech. Discuss., https://doi.org/10.5194/amt-2017-214
Manuscript under review for journal Atmos. Meas. Tech.
Discussion started: 17 July 2017

Atmospheric Measurement Techniques Discussions

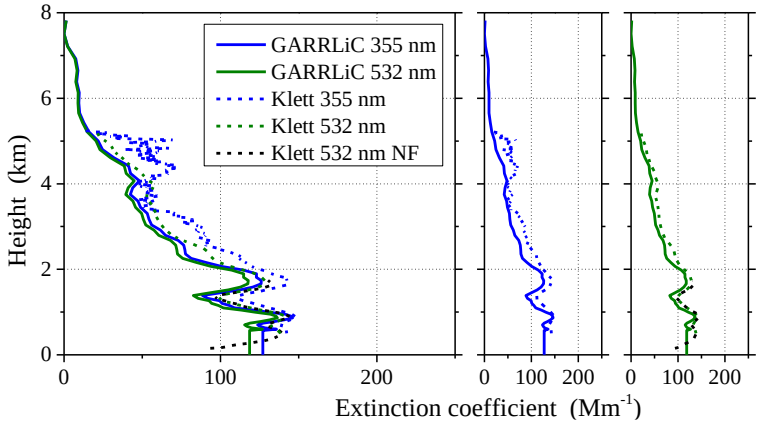

Figure 4: Backscatter and extinction coefficient retrievals, at Finokalia, Crete, on June 26, 2014, at 04:00-06:00 UTC. First and second rows: Backscatter and extinction coefficients from GARRLiC and LIRIC. Third and fourth rows: Backscatter and extinction coefficients from GARRLiC and Klett. In each row the first plot contains the results for all wavelengths (i.e., 355, 532 and 1064 nm) and the next three plots contain the results for each wavelength separately.

Atmos. Meas. Tech. Discuss., https://doi.org/10.5194/amt-2017-214
Manuscript under review for journal Atmos. Meas. Tech.
Discussion started: 17 July 2017

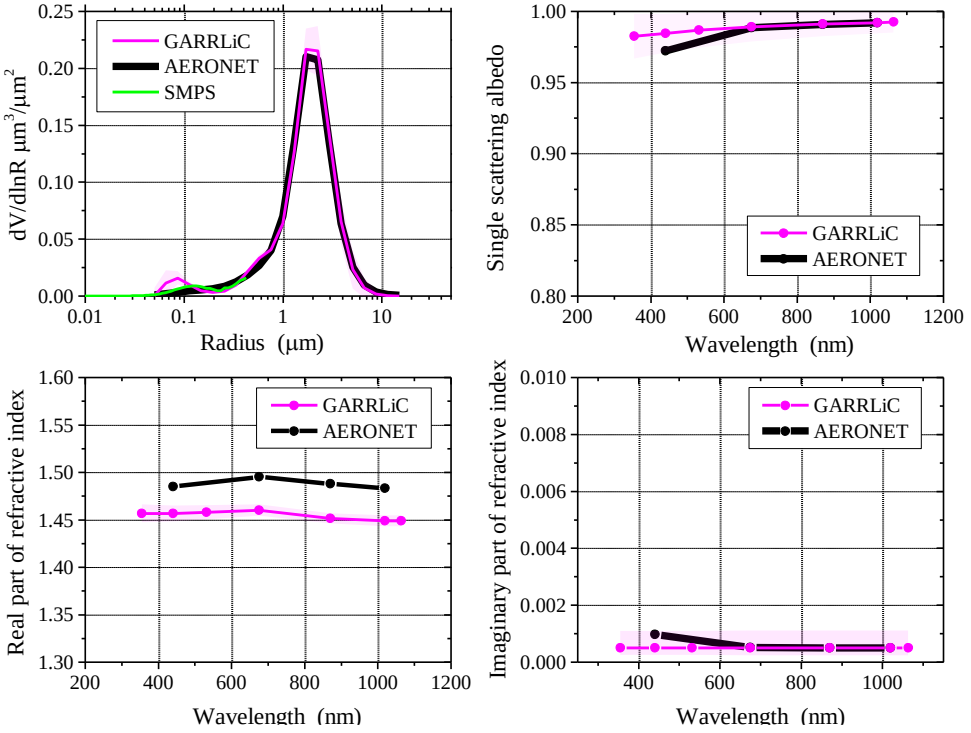

Figure 5: GARRLiC retrievals (pink) of size distribution (up-left), spectral SSA (up-right), spectral real and imaginary part of the refractive index (bottom –left and right), on June 26, 2014, at 04:00-06:00 UTC, in Finokalia, Crete. The black line shows the AERONET retrieval at 04:54 UTC (used also in LIRIC). The green line in the size distribution plot (up-left) is the mean value of the surface in situ SMPS measurements at 04:00-06:00 UTC.

Atmos. Meas. Tech. Discuss., https://doi.org/10.5194/amt-2017-214
Manuscript under review for journal Atmos. Meas. Tech.
Discussion started: 17 July 2017

Atmospheric Measurement Techniques Discussions

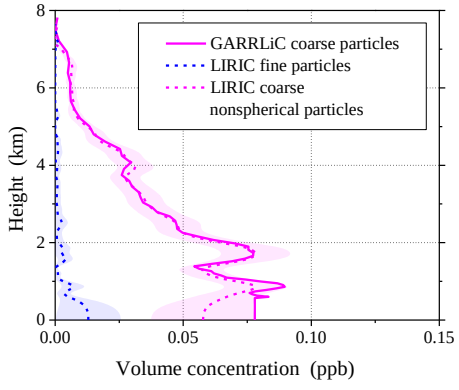

a)

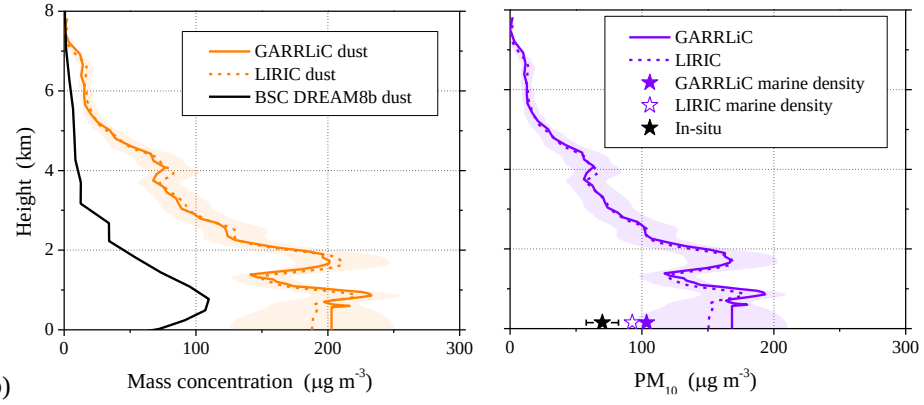

b)

Figure 6: a) Volume concentration profiles for GARRLiC coarse particles (pink), and LIRIC fine (dash blue) and coarse nonspherical particles (dash pink), on June 26, 2014, at 04:00-06:00 UTC, in Finokalia, Crete. b) Left: Dust mass concentration profiles from GARRLiC (orange), LIRIC (dash orange) and BSC DREAM8b model (black) (the latter at 05:00 UTC). Right: PM_{10} profiles from GARRLiC (purple) and LIRIC (dash purple), along with their surface values, considering only marine particles at the surface ("GARRLiC marine density" and "LIRIC marine density" denoted by purple star and white star, respectively). The black star denotes the surface in situ measurements at 05:00-06:00 UTC (mean and time variability).

Atmos. Meas. Tech. Discuss., https://doi.org/10.5194/amt-2017-214
Manuscript under review for journal Atmos. Meas. Tech.
Discussion started: 17 July 2017

Atmospheric Measurement Techniques Discussions

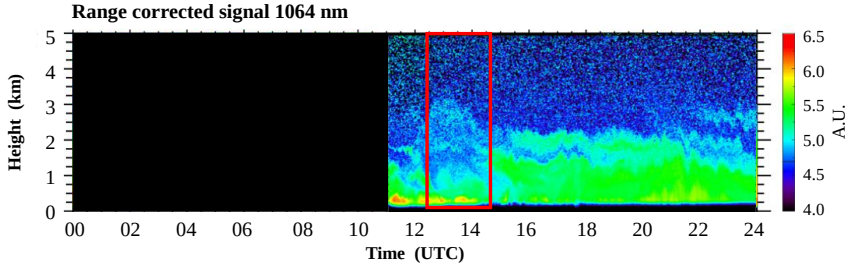

a)

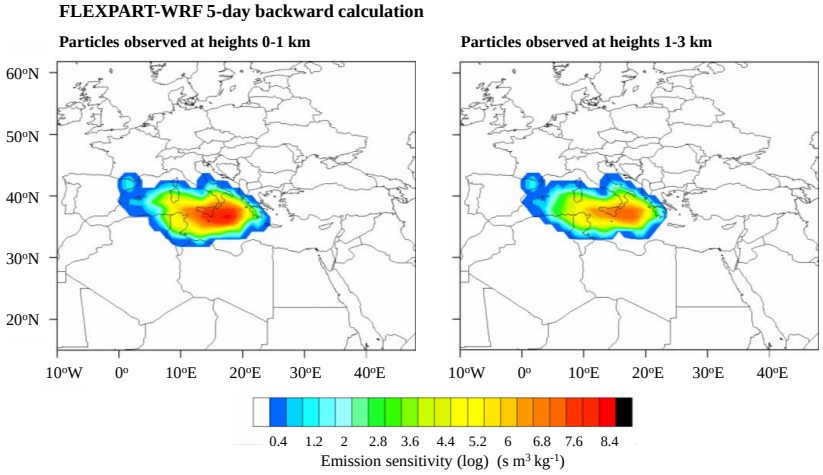

b)

Figure 7. a) Range-corrected backscattered signal at 1064 nm in arbitrary units from Polly^{XT} OCEANET lidar, at Finokalia, Crete, on July 15, 2014. The red rectangle indicates the time range of the measurements used for the GARRLiC and LIRIC retrievals (12:30-14:30 UTC). b) Five day backward FLEXPART-WRF calculation of emission sensitivity (i.e., residence time in the lowest 1 km in the atmosphere) in log(s m^3 kg^{-1}) for the particles arriving at the layers 0-1 km (left) and 1-3 km (right) at 14:00 UTC.

Atmos. Meas. Tech. Discuss., https://doi.org/10.5194/amt-2017-214
Manuscript under review for journal Atmos. Meas. Tech.
Discussion started: 17 July 2017

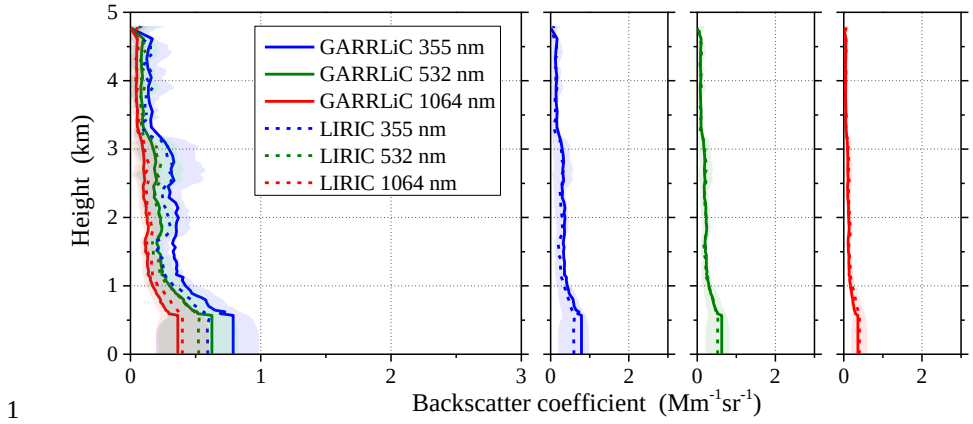

1

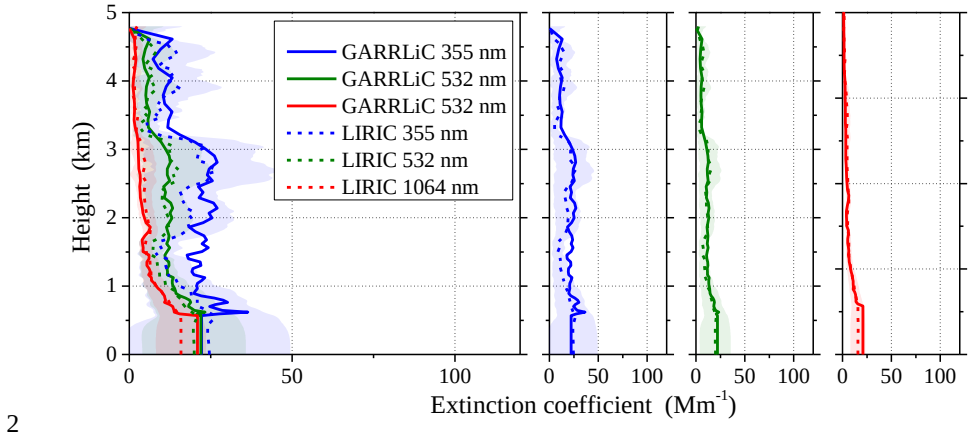

2

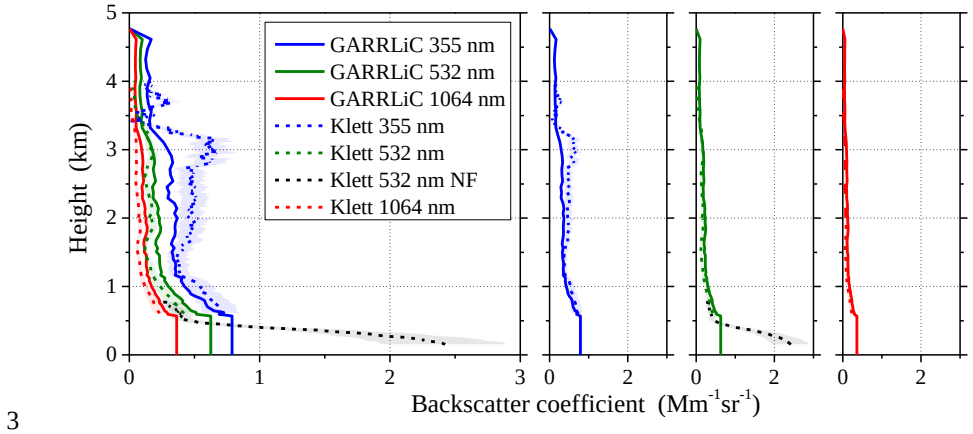

3

Atmos. Meas. Tech. Discuss., https://doi.org/10.5194/amt-2017-214
Manuscript under review for journal Atmos. Meas. Tech.
Discussion started: 17 July 2017

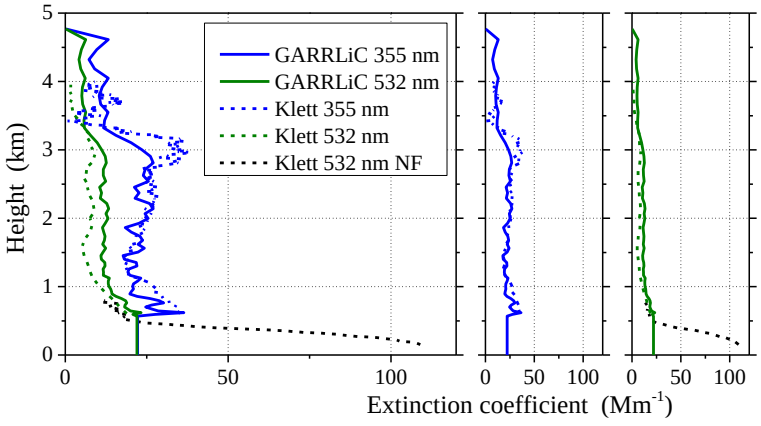

Figure 8: As in Fig. 4 for backscatter and extinction coefficient retrievals at Finokalia, Crete, on July 15, 2014, at 12:30-14:30 UTC.

Atmos. Meas. Tech. Discuss., https://doi.org/10.5194/amt-2017-214
Manuscript under review for journal Atmos. Meas. Tech.
Discussion started: 17 July 2017

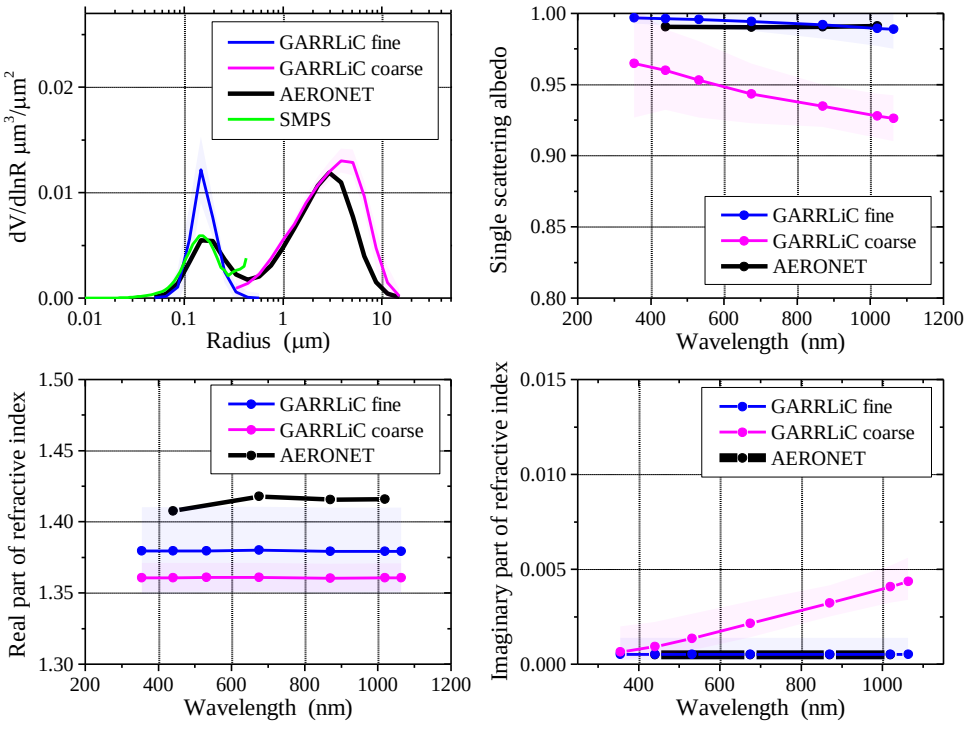

Figure 9: GARRLiC retrievals for fine (blue) and coarse particles (pink) of size distribution (up-left), spectral SSA (up-right), spectral real and imaginary part of the refractive index (bottom –left and right), at Finokalia, Crete, on July 15, 2014, at 12:30-14:30 UTC. The black line shows the AERONET retrieval at 13:24 UTC. The green line in the size distribution plot (up-left) is the mean value of the surface in situ SMPS measurements at 12:00-13:20 UTC.

Atmos. Meas. Tech. Discuss., https://doi.org/10.5194/amt-2017-214
Manuscript under review for journal Atmos. Meas. Tech.
Discussion started: 17 July 2017

Atmospheric Measurement Techniques Discussions

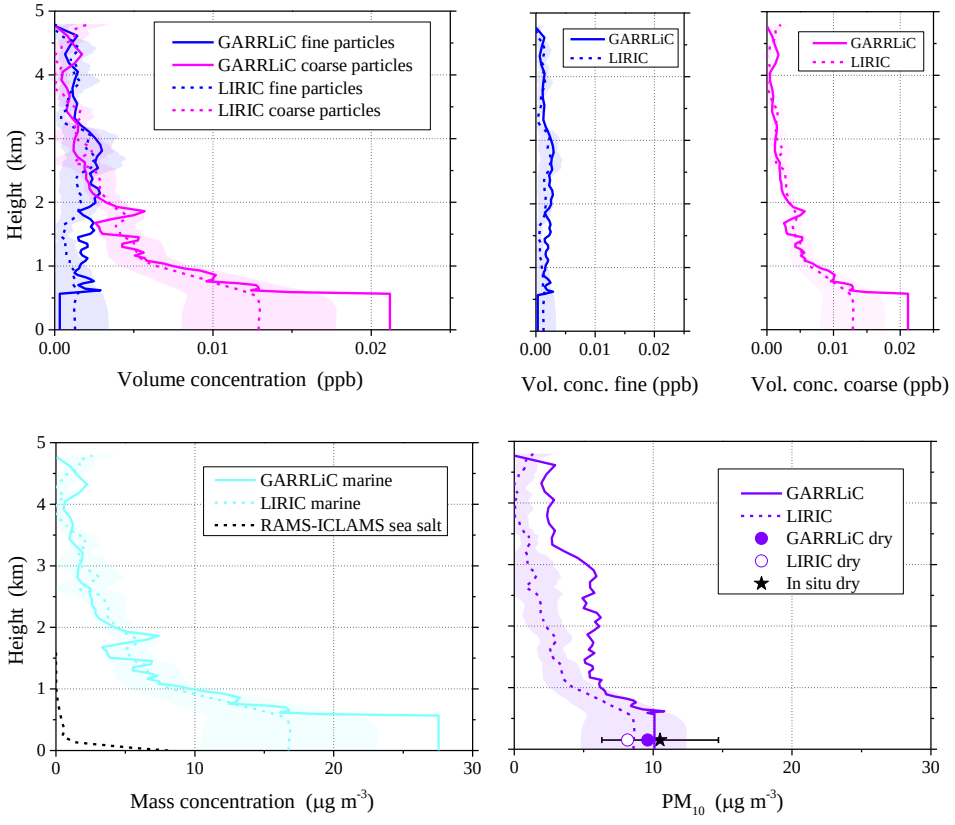

Figure 10: a) Volume concentration profiles for GARRLiC fine (blue) and coarse particles (pink) and LIRIC fine (dash blue) and coarse spherical particles (dash pink), at Finokalia, Crete, on July 15, 2014, at 12:30-14:30 UTC. b) Left: GARRLiC (light blue) and LIRIC (dash light blue) marine particle mass concentration profiles, along with the RAMS-ICLAMS sea salt mass concentration profile (black) at 13:00 UTC. Right: PM_{10} profiles from GARRLiC (purple) and LIRIC (dash purple), along with the "dry" GARRLiC and LIRIC PM_{10} at the surface (purple and white circles, respectively). The black star denotes the in situ PM_{10} measurements at 4-5 UTC (mean and time variability).

Atmos. Meas. Tech. Discuss., https://doi.org/10.5194/amt-2017-214
Manuscript under review for journal Atmos. Meas. Tech.
Discussion started: 17 July 2017

Atmospheric Measurement Techniques Discussions

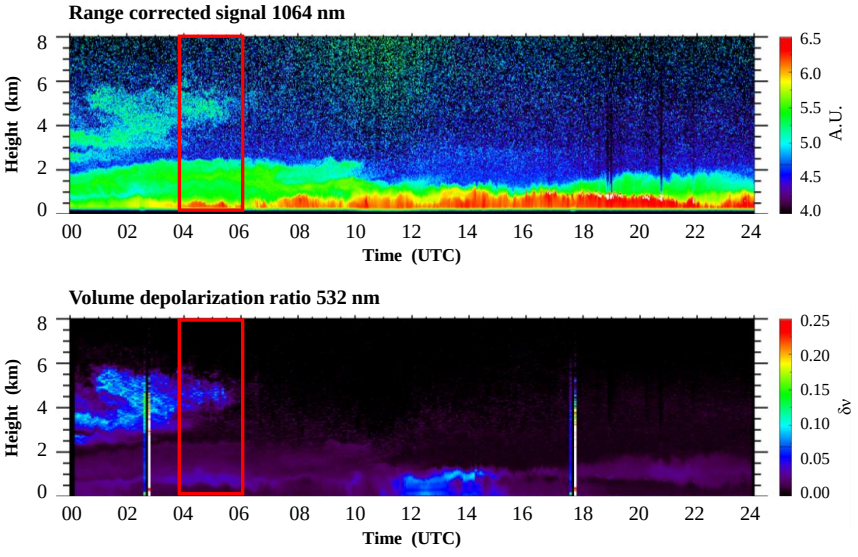

a)

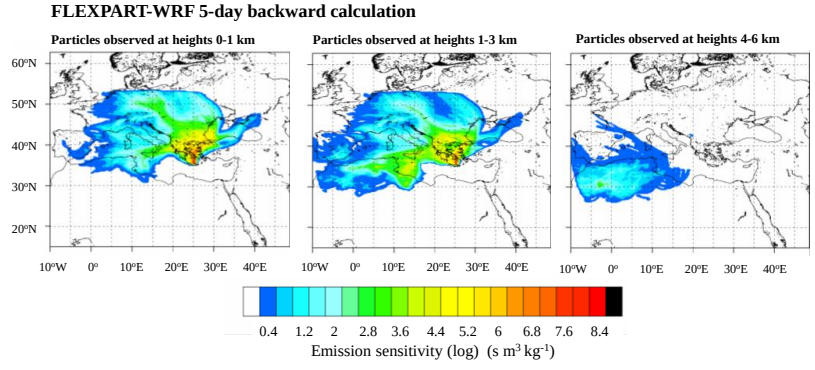

b)

Figure 11: a) Range-corrected backscattered signal at 1064 nm in arbitrary units (top) and volume depolarization ratio at 532 nm (bottom) from Polly^{XT} OCEANET lidar, at Finokalia, Crete, on July 4, 2014. The red rectangle indicates the GARRLiC and LIRIC retrievals (04:00-06:00 UTC). b) Five day backward FLEXPART-WRF calculation of emission sensitivity (i.e., residence time in the lowest 1km in the atmosphere) in log(s m^3 kg^{-1}) for the particles arriving at heights 0-1 km (left), 1-3 km (middle) and 4-6 km (right), at 07:00 UTC.

Atmos. Meas. Tech. Discuss., https://doi.org/10.5194/amt-2017-214
Manuscript under review for journal Atmos. Meas. Tech.
Discussion started: 17 July 2017

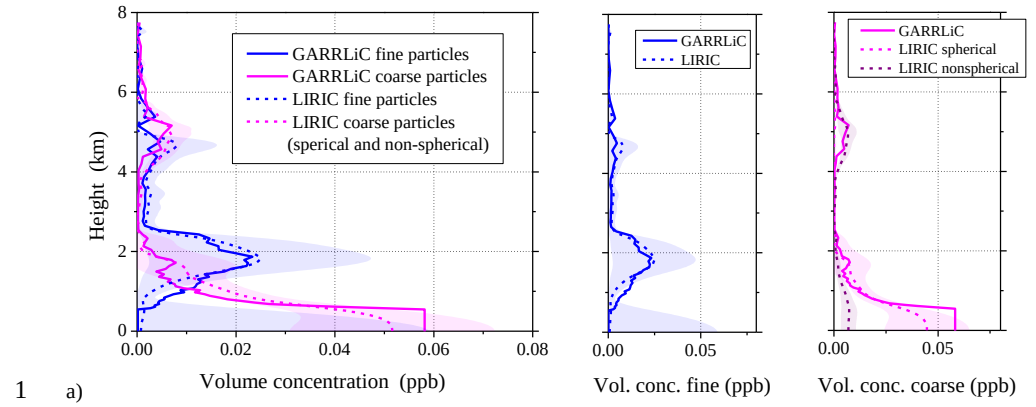

a)

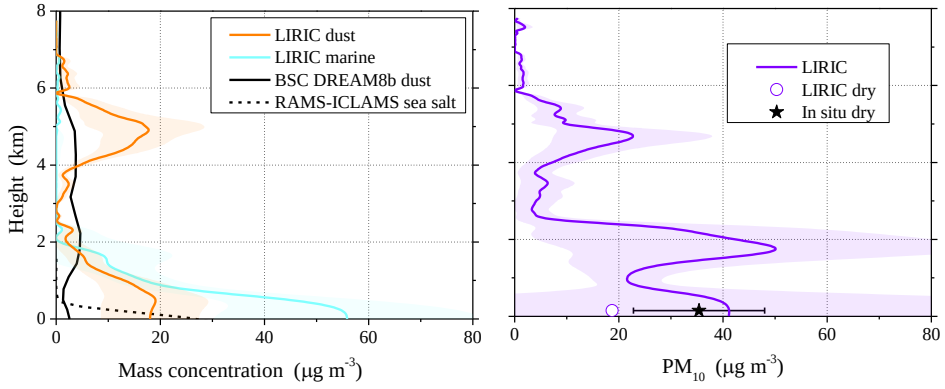

b)

Figure 12: a) Left: Volume concentration profiles for GARRLiC fine (blue) and coarse particles (pink) and LIRIC fine (dash blue) and total coarse particles (dash pink), at Finokalia, Crete, on July 4, 2014, at 04:00-06:00 UTC. Middle: Volume concentration of fine particles from GARRLiC (blue) and LIRIC (dash blue). Right: Volume concentration of coarse particles from GARRLiC (pink) and LIRIC, disentangled in the spherical (dash pink) and non-spherical (dash purple) components. b) Left: Mass concentration profiles for LIRIC dust (orange) and marine particles (light blue), along with the modelled dust (black) and sea salt (dash black) particle concentration profiles (both at 05:00 UTC). Right: PM_{10} profile from LIRIC (purple), along with the "dry" LIRIC PM_{10} at the surface (white circle). The black star denotes the surface in situ PM_{10} measurements at 4-5 UTC (mean and time variability).

Atmos. Meas. Tech. Discuss., https://doi.org/10.5194/amt-2017-214
Manuscript under review for journal Atmos. Meas. Tech.
Discussion started: 17 July 2017

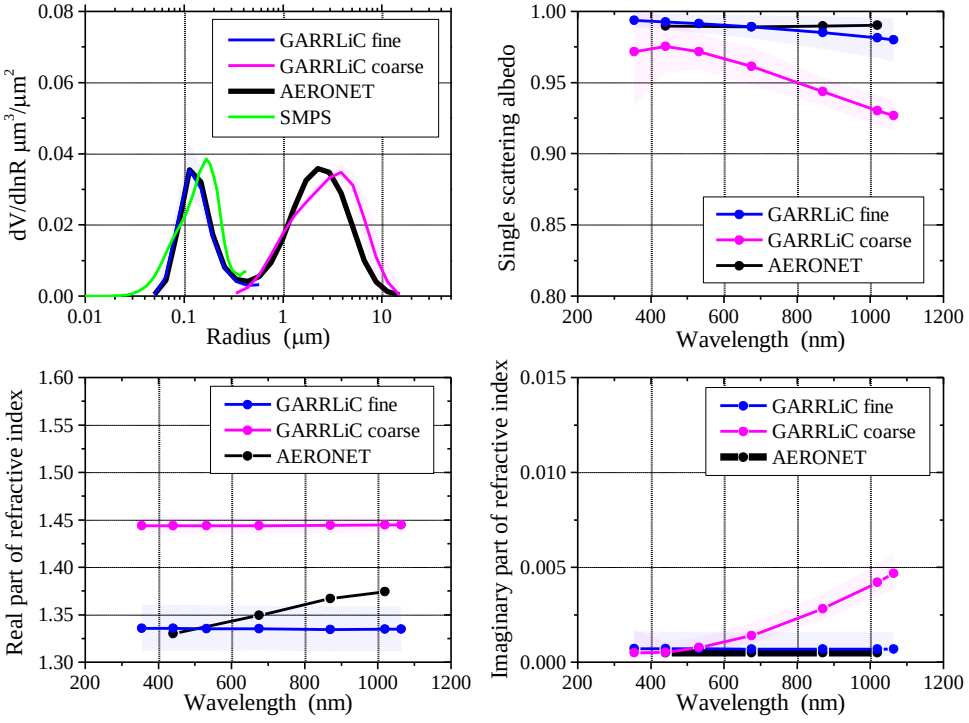

Figure 13: GARRLiC retrievals for fine (blue) and coarse particles (pink) of size distribution (up-left), spectral SSA (up-right), spectral real and imaginary part of the refractive index (bottom –left and right), at Finokalia, Crete, on July 4, 2014, at 04:00-06:00 UTC. The black line shows the AERONET retrieval at 05:49 UTC. The green line in the size distribution plot (up-left) is the mean value of the surface in situ SMPS measurements at 04:00-06:00 UTC.

Atmos. Meas. Tech. Discuss., https://doi.org/10.5194/amt-2017-214
Manuscript under review for journal Atmos. Meas. Tech.
Discussion started: 17 July 2017

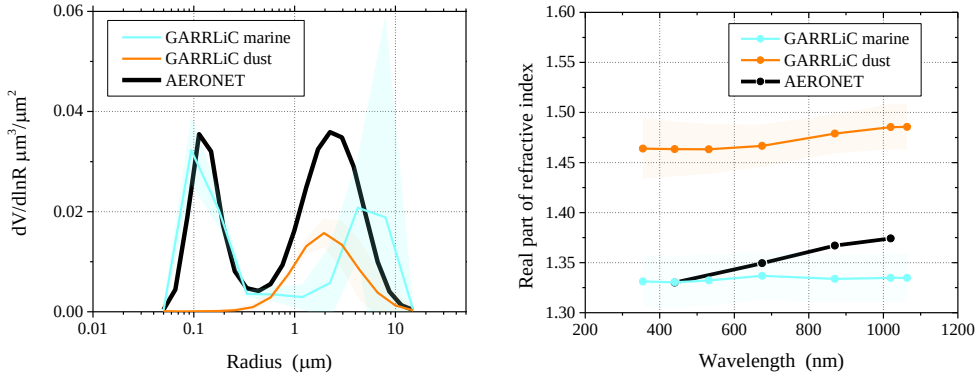

Figure 14: Potential of GARRLiC to retrieve "marine" (light blue) and "dust" particle (orange) size distribution (left) and spectral real part of the refractive index (right). The retrieval refers to measurements at Finokalia, Crete, on July 4, 2014, at 04:00-06:00 UTC. The black line shows the AERONET retrieval at 05:49 UTC.

Atmos. Meas. Tech. Discuss., https://doi.org/10.5194/amt-2017-214
Manuscript under review for journal Atmos. Meas. Tech.
Discussion started: 17 July 2017

Atmospheric Measurement Techniques Discussions

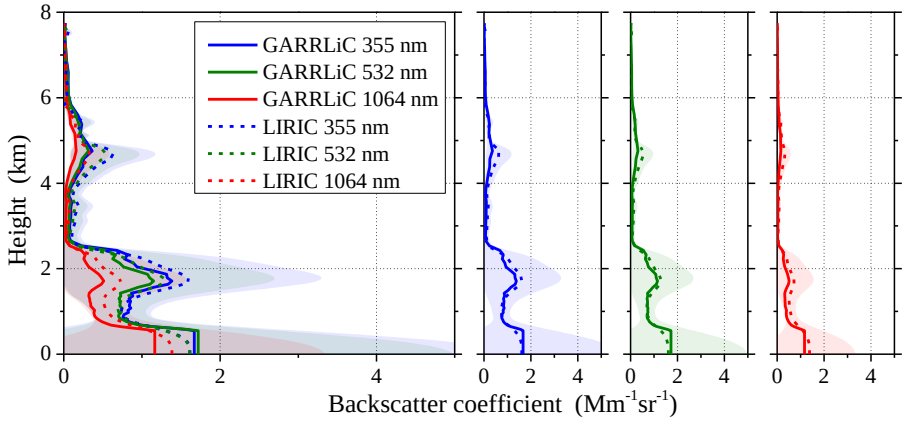

1

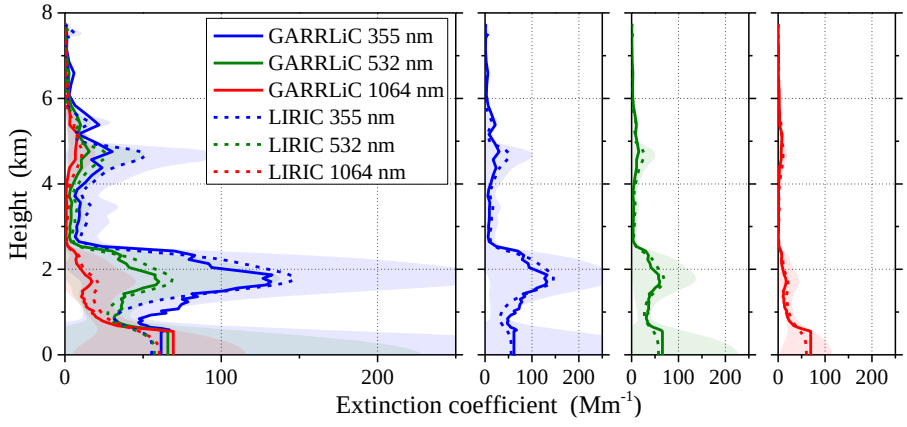

2

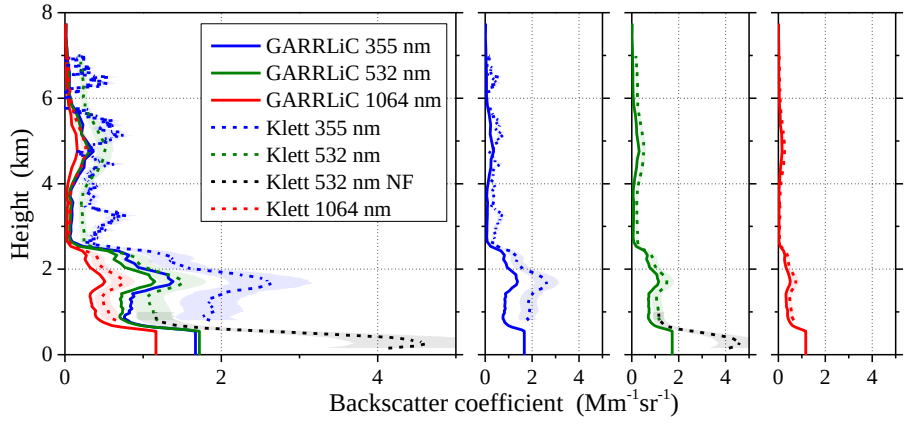

3

Atmos. Meas. Tech. Discuss., https://doi.org/10.5194/amt-2017-214
Manuscript under review for journal Atmos. Meas. Tech.
Discussion started: 17 July 2017

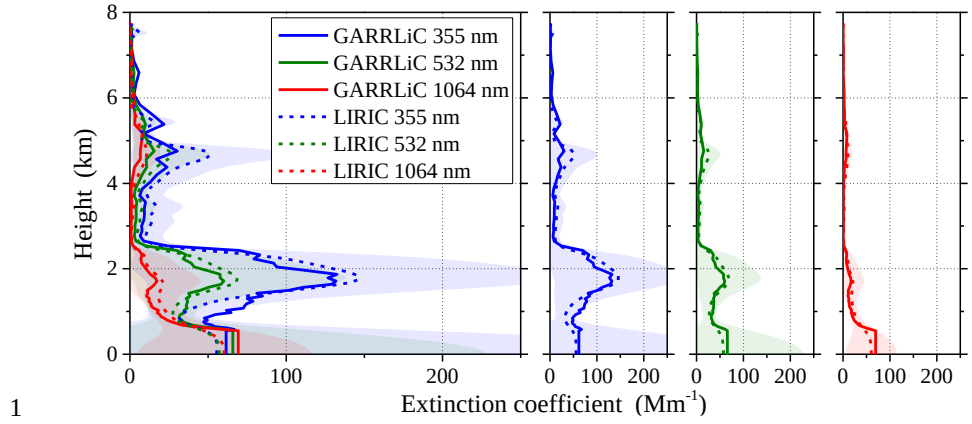

Figure 15: As in Fig. 4 for backscatter and extinction coefficient retrievals at Finokalia, Crete, on July 4, 2014, at 04:00-06:00 UTC.